

EFFECT OF TEMPERATURE ON FATIGUE PROPERTIES OF
DIN 35 NiCrMoV 12 5 STEEL

A THESIS SUBMITTED TO
THE GRADUATE SCHOOL OF NATURAL AND APPLIED SCIENCES
OF
THE MIDDLE EAST TECHNICAL UNIVERSITY

BY

ORKUN UMUR ÖNEM

IN PARTIAL FULFILLMENT OF THE REQUIREMENTS FOR THE DEGREE OF
MASTER OF SCIENCE
IN
THE DEPARTMENT OF METALLURGICAL AND MATERIALS ENGINEERING

JULY 2003

Approval of the Graduate School of Natural and Applied Sciences.

Prof. Dr. Canan ÖZGEN
Director

I certify that this thesis satisfies all the requirements as a thesis for the degree of Master of Science.

Prof. Dr. Bilgehan ÖGEL
Head of Department

We certify that we have read this thesis and in our opinion it is fully adequate, in scope and quality, as a thesis for the degree of Master of Science in Metallurgical and Materials Engineering.

Assoc. Prof. Dr. Rıza GÜRBÜZ
Supervisor

Examining Committee Members:

Prof. Dr. Bilgehan ÖGEL

Prof. Dr. Vedat AKDENİZ

Assoc. Prof. Dr. Hakan GÜR

Assoc. Prof. Dr. Rıza GÜRBÜZ

Assoc. Prof. Dr. A. Tamer ÖZDEMİR

ABSTRACT

EFFECT OF TEMPERATURE ON FATIGUE PROPERTIES OF DIN 35 NiCrMoV 12 5 STEEL

Önem, Orkun Umur

M.Sc., Department of Metallurgical and Materials Engineering

Supervisor: Assoc. Prof. Dr. Rıza Gürbüz

July 2003, 73 pages

DIN 35NiCrMoV125 (equivalent to AISI 4340), which is a high strength low alloy steel (HSLA), is mainly used at military applications in the production of gun barrels. The main aim of this study was to determine the low cycle fatigue (LCF) behaviour and the influence of temperature on low cycle fatigue failure properties of that steel.

Three different temperatures (room temperature, 250⁰C and 400⁰C) were used in the experiments in order to analyze the effect of temperature. For each temperature, five strain amplitudes (in the range of 0.2% offset yield point to 2% strain) were applied and the duplicates of each experiment were performed to obtain more accurate results. Strain amplitudes and the corresponding stresses were calculated from tension tests performed at each temperature. Strain amplitude versus fatigue life (e-

N) curves for three different temperatures predicted that fatigue life at a given strain increases with increasing temperature. The transition lives of those three curves were observed at 1 % strain amplitude and no significant effect of temperature on transition lives was observed. For stress based analysis, stress versus fatigue life (S-N) curves were drawn. These curves pointed that fatigue strength at a given number of cycle decreases with increasing temperature.

Fractographic analyses of the fracture surfaces were performed to examine the effects of load and temperature on the specimens. It was observed that the number of crack initiation sites increases with increasing strain.

Keywords: DIN 35NiCrMoV125 Steel, AISI 4340 Steel, Low Cycle Fatigue, e-N, S-N, Temperature, Fractography.

ÖZ

DIN 35 NiCrMoV 12 5 ÇELİĞİNDE SICAKLIĞIN YORULMA ÖZELLİĞİ ÜZERİNE ETKİSİ

Önem, Orkun Umur

Yüksek Lisans, Metalurji ve Malzeme Mühendisliği Bölümü

Tez Yöneticisi: Assoc. Prof. Dr. Rıza Gürbüz

Temmuz 2003, 73 sayfa

Düşük alaşımlı, yüksek dayanımlı DIN 35NiCrMoV125 çelikleri (yaklaşık karşılığı AISI 4340) savunma sanayiinde genel olarak namlu yapımında kullanılır. Bu çalışmanın asıl amacı, namlu çeliklerinde, sıcaklığın malzemenin düşük çevrimli yorulma özellikleri üzerine etkisini incelemektir.

Sıcaklığın yorulma davranışı üzerine olan etkisini açıklayabilmek için oda sıcaklığı, 250⁰C ve 400⁰C olmak üzere üç sıcaklık seçildi. Her sıcaklık için, malzemenin %0.2 offset akma dayancı ve %2 gerinim aralığında, beş yük kullanıldı ve sonuçların güvenilirliği açısından her deney koşulu iki kez tekrar edildi. Kullanılan gerilim genlikleri her sıcaklıkta yapılan çekme deneylerinin sonuçlarına göre belirlendi. Gerinim genliği – yorulma ömrü (e-N) eğrileri karşılaştırıldığında belirli bir gerinim genliğindeki yorulma

ömrünün sıcaklıkla arttığı görüldü. Her üç eğrinin için geçiş ömrünün %0.1 gerinim genliğine karşılık geldi ve sıcaklığın geçiş ömrüne önemli derecede etki etmediği gözlemlendi. Gerilim değerlerine dayanılarak yapılan çalışma için gerilim – yorulma ömrü (S-N) grafiklerinden yararlanıldı. Sıcaklık arttıkça yorulma dayancının azaldığı görüldü.

Kırılma yüzeylerinde yük ve sıcaklıktan dolayı oluşan değişimleri inceleyebilmek için fraktografi metodu kullanıldı. Uygulanan yük arttıkça yüzeyde oluşan çatlak sayısının da arttığı görüldü.

Anahtar Kelimeler: DIN 35NiCrMoV125 Çeliği, AISI 4340 Çeliği, Düşük Çevrimli Yorulma, e-N, S-N, Sıcaklık, Fraktografi.

To my family

ACKNOWLEDGEMENTS

I would like to thank Assoc. Prof. Dr. Rıza GÜRBÜZ for all the support and advice that he provided me throughout this thesis study.

Also, I would like to thank research assistant Nevzat AKGÜN for his help in preparing the experimental setup that I used.

I would like to express my thanks to Fatih GÜNER, İlker KAŞIKÇI and SÜHA TİRKEŞ for all their support.

Finally, thanks to Burcu MANAV for her encouragement in reaching the end at my study.

TABLE OF CONTENTS

ABSTRACT	iii
ÖZ	v
DEDICATION	vii
ACKNOWLEDGEMENTS	viii
TABLE OF CONTENTS	ix
LIST OF TABLES	xii
LIST OF FIGURES	xiii
CHAPTER	
1. INTRODUCTION	1
2. THEORY	5
2.1. The History of Fatigue	5
2.2. Basic Factors of Fatigue Failure	6
2.3. Fatigue Life	8
2.3.1. Factors Affecting Fatigue Life	8
2.3.1.1. Effects of Material Condition on Fatigue	9
2.3.1.2. Effects of Manufacturing Practices on Fatigue	9
2.4. The S-N Curve	10
2.5. Gun Barrel Fatigue Process	11
2.6. Effect of Temperature on Fatigue Failure	12
2.6.1. The Stress-Endurance Curve At Different Temperatures	13

2.6.2.	The Fatigue Strength Of Steels At High Temperatures And Comparison With Other Mechanical Properties	14
2.6.3.	Effect of Testing Frequency	16
2.6.4.	Effect of Metallographic Structure	17
2.6.5.	Effect of Plastic Deformation During Fatigue	19
2.7.	Fatigue Crack Propagation	20
2.7.1.	Influence of Temperature on Fatigue Crack Propagation	23
2.7.2.	Fatigue Crack Propagation Rate	24
2.8.	High Cycle versus Low Cycle Fatigue	25
2.8.1.	Low Cycle (Cyclic Strain-Controlled) Fatigue	25
2.8.1.1.	Cycle-Dependent Material Response.....	25
2.8.1.2.	Strain Life Curves	28
2.8.1.3.	Effect of Surface Treatment on Low Cycle Fatigue	30
3.	EXPERIMENTAL PROCEDURE	31
3.1.	Material	31
3.2.	Testing Specimen	33
3.3.	Fatigue Life Testing	34
3.4.	Fractography	40
4.	RESULTS AND DISCUSSIONS	42
4.1.	Tension and Fatigue Test Results for RT, 250 ⁰ C and 400 ⁰ C	43
4.2.	Fatigue Strength and Fatigue Ductility Curves	46
4.3.	Elastic to Plastic Transition Life	49
4.4.	Strain Amplitude versus Fatigue Life Curves	51
4.4.1.	Room Temperature S – N Curve	51

4.4.2.	250 ⁰ C S – N Curve	52
4.4.3.	400 ⁰ C S – N Curve	52
4.5.	Stress versus Fatigue Life (S-N) Curves	53
4.6.	Effect of Temperature on Fatigue Life Results ...	54
4.6.1.	Temperature – Fatigue Life Correlation by Fatigue Damage Equations	58
4.6.2.	Temperature – Fatigue Life Correlation by Experimental Results	60
4.7.	Fractographic Results	61
4.7.1.	Macro Inspection	61
4.7.2.	Micro Inspection	65
5.	CONCLUSIONS	71
	REFERENCES	72

LIST OF TABLES

TABLES

3.1	Weight Percentages of Testing Material	32
3.2	Material Properties of AISI 4340 Steel_Ref. [10]	32
3.3	Fracture Toughness Value of Testing Material	32
3.4	Room Temperature Strain and Load Values	35
3.5	Room Temperature S_{max} , S_{min} and S_a Values	36
3.6	250 ⁰ C Strain and Load Values	36
3.7	250 ⁰ C S_{max} , S_{min} and S_a Values	36
3.8	400 ⁰ C Strain and Load Values	36
3.9	400 ⁰ C S_{max} , S_{min} and S_a Values	37
4.1	Room Temperature Mechanical Properties	44
4.2	250 ⁰ C Mechanical Properties	44
4.3	400 ⁰ C Mechanical Properties	44
4.4	Room Temperature Fatigue Experiments	45
4.5	250 ⁰ C Fatigue Experiments	45
4.6	400 ⁰ C Fatigue Experiments	46
4.7	Comparison of Experimental Transition Lives	49
4.8	Results of all Fatigue Experiments	56
4.9	Comparison of Exp. and Calc. Results by Damage Equations	59
4.10	Fatigue Lives Calculated by Polynomial Equations	61

LIST OF FIGURES

FIGURES

1.1	Fractured Gun Tube [1]	3
2.1	Axial, Torsional and Flexural Stresses [3]	7
2.2	Typical S-N Curves [4]	10
2.3	High Temperature S-N Curve for 0.17% C Steel at 400 ⁰ C [6]	13
2.4	High Temperature Mechanical Properties for 0.17% C Steel at 400 ⁰ C [6]	15
2.5	Frequency Effect on Fatigue Life of 0.17% C Steel at 400 ⁰ C [5]	17
2.6	Effect of Grain Size at Ferrovac Iron [7]	18
2.7	Effect of Plastic Deformation at Mild Steels [6]	20
2.8	Phases of Fatigue Failure [4]	21
2.9	Beachmarks or “Clamshell Pattern” [4]	22
2.10	Example of the Striations Found in Fatigue Fracture [4]	23
2.11	Cycle-dependent Material Response under Stress Control [1]	26
2.12	Cycle-dependent Material Response under Strain Control [1]	26
2.13	Hysteresis Loop [1]	27
2.14	Strain-Life Curve [1]	30
3.1	Microstructure of As-Recieved DIN 35NiCrMoV125 Steel, a) in L-R direction, b) in R-L direction	33

3.2	Dimensions of Testing Specimen	33
3.3	Orientation of Specimen	34
3.4	Haver Sine Wave	35
3.5	Furnace Attached to MTS Testing Machine	38
3.6	Position of Thermocouple	39
3.7	The Whole Setup	40
4.1	Engineering Stress (σ) versus Engineering Strain (ϵ) diagrams for RT, 250 ⁰ C and 400 ⁰ C	43
4.2	Fatigue Strength Properties	47
4.3	Fatigue Ductility Properties	48
4.4	Transition Life at RT	50
4.5	Transition Life at 250 ⁰ C	50
4.6	Transition Life at 400 ⁰ C	51
4.7	Strain - Life Curves at Three Temperatures	52
4.8	Stress - Life Curves at Three Temperatures	54
4.9	Microstructure of Specimen After Fatigue Test at 400 ⁰ C and 0.2% Strain Amplitude (50X)	55
4.10	Temperature versus Total Life	61
4.11	Crack initiation sites (encircled regions) at RT and 2 % strain amplitude	62
4.12	Crack initiation sites (encircled regions) at 250 ⁰ C and 2 % strain amplitude	62
4.13	Crack initiation sites (encircled regions) at 400 ⁰ C and 2 % strain amplitude	63
4.14	Crack initiation site at 250 ⁰ C & 0.2 % strain amplitude	64
4.15	Crack initiation site at 400 ⁰ C & 0.2 % strain amplitude	64
4.16	Crack initiation at 250 ⁰ C and 0.2 % strain	65
4.17	Crack initiation at 400 ⁰ C and 0.2 % strain	66

4.18	Tear ridges and secondary crack at 250 ⁰ C and 0.2 % strain	67
4.19	Striations and secondary cracks at 250 ⁰ C and 2 % strain	67
4.20	Striations formed at 250 ⁰ C and 2 % strain	68
4.21	Striations formed at 400 ⁰ C and 2 % strain	69
4.22	Dimples formed at 250 ⁰ C and 0.2 % strain	70
4.23	Dimples formed at 400 ⁰ C and 0.2 % strain	70

CHAPTER 1

INTRODUCTION

Purely static loading is rarely observed in modern engineering components or structures. By far, the majority of structures involve parts subjected to fluctuating or cyclic loads. For this reason, design analysts must address themselves to the implications of repeated loads, fluctuating loads, and rapidly applied loads. Such loading induces fluctuating or cyclic stresses that often result in failure of the structure by fatigue. Indeed, it is often said that from 80% to 95% of all structural failures occur through a fatigue mechanism.

It is next to impossible to detect any progressive changes in material behavior during the fatigue process, and therefore failures often occur without warning. Also, periods of rest with the fatigue stress removed do not lead to any measurable healing or recovery of the material. Thus, the damage done during the fatigue process is cumulative, and generally unrecoverable.

Steel is one of the most important materials in engineering and structural applications because of its high toughness, high strength and other outstanding mechanical properties compared with other materials. The material that will be observed in this report is DIN 35 NiCrMoV 12 5 steel which has a similar composition with AISI 4340 steel. So, literature survey is done over these two steels. DIN 35 NiCrMoV 12 5 steel is used mainly in the production of gun barrels used by Turkish Army Forces. This

is a heat treatable, high strength low alloy steel (HSLA) containing nickel, chromium, molybdenum and vanadium as the main alloying elements. It is known for its high toughness and capability of developing high strength in the heat treated condition while retaining good fatigue strength. Typical applications, beside gun barrel production, are for structural use, such as aircraft landing gear, power transmission gears and shafts and other structural parts. This ultra high strength low alloy steel, especially, is preferred in weapon and aerospace industries and in these fields the reliability is mandatory in service conditions. Since high toughness is required in those fields, AISI 4340 should be purified with some special refining processes with care. Although very good microstructure properties are gained with these processes, AISI 4340 may suddenly fail under different kinds of service conditions, temperatures and cyclic loads.

Fatigue is an important failure criterion for a gun barrel. During the firing process of a gun barrel, heat checks, also known as crack initiation sites, are formed. These are small, sometimes invisible to the naked eye, cracks in the surface of the bore. The formation of those small crack initiation sites may also start to occur after firing approximately 300 rounds. A gun barrel, manufactured from a high strength steel alloy for U.S. Army, was failed catastrophically and broke into 29 pieces (Fig. 1.1). As mentioned above, crack initiation was believed to have occurred on the inner bore of the gun tube from a thermally induced cracking known as heat checking [1].

Once the heat checks or cracks are formed, a random network of cracks penetrate below the inner surface of the bore. These cracks continue to grow slowly under the influence of stresses in the gun barrel and they come in contact with the hot combustion gases occur during the firing process. Heat checks will then connect together to form longitudinal and circumferential cracks. Those cracks are then propagate until failure occurs. If one round is assumed as one cycle, the propagation of these cracks reflect fatigue crack propagation property.



Figure 1.1 Fractured Gun Tube [1]

In addition, the hot combustion gases occur during the firing process increases the temperature of the gun barrel. This increase in temperature may also effect the life of component in terms of corrosion, temper embrittlement etc.

Fatigue is encountered in several ways. One source is vibration as a consequence of rotation, or of fluid motion, and failure may result after a large number of cycles. Another source of fatigue is a consequence of start and stop operation, and is identified generally as thermal or low cycle fatigue. Here, strain is the controlling variable.

High temperature introduces a number of complications. Included are:

a. Gaseous or liquid environments introduce surface reactions which interact strongly with fatigue cracks to accelerate crack initiation, growth and failure.

b. Long hold-time period between cycles introduce creep effects which interact with fatigue, often by changing the mode of crack propagation from the more ductile transgranular mode to the more brittle intergranular type.

c. The material may change its properties with long times at temperature due to aging and phase instability effects or to creep damaging mechanisms.

d. Thermal cycling introduces complications regarding predictions of stresses and strains and uncertainty regarding the interaction of temperature cycling and strain cycling.

In the light of those reasons, it can be concluded that the failure of a gun barrel will not exceed 10^5 cycles. Since 10^5 cycles is assumed to be the limit between high cycle fatigue and low cycle fatigue, this report is based on the low cycle properties rather than high cycle fatigue. As a result, the fatigue term in elevated temperatures for DIN 35 NiCrMoV 12 5 steel should be considered as an important phenomena.

CHAPTER 2

THEORY

2.1. The History of Fatigue

For centuries, it has been known that a piece wood or metal can be made to break by repeatedly bending it back and forth with a large amplitude. However, it came as something of a surprise when it was discovered that repeated loading produced fracture even when the stress amplitude was apparently well below the elastic limit of the material. The first fatigue investigations seemed to have been reported by a German mining engineer, W. A. S. Albert, who in 1829, performed some repeated loading tests on iron chain. Some of the earliest fatigue failures in service, occurred in the axles of stage coaches. When railway systems began to develop rapidly in the middle of the nineteenth century, fatigue failures of railway axles became a widespread problem that began to draw attention to cyclic loading effects. This was the first time that many similar components had been subjected to millions of cycles at stress levels well below the monotonic tensile yield stress. As is often the case with unexplained service failures, attempts were made to reproduce the failures in the laboratory. Between 1852 and 1870, the German railway engineer August Wohler setup and conducted the first systematic fatigue investigation. From this point of view, he may be regarded as the grandfather of modern fatigue thinking. He conducted tests on full-scale railway axles and also on small scale bending, torsion, and axial cyclic

loading specimens for different materials. Some of Wohler's data for Krupp axle steel were plotted in terms of nominal stress amplitude versus cycles to failure. This presentation of fatigue life has become very well known as the S-N diagram. Each curve on such a diagram is still referred to as a Wohler line [2].

At about the same time, other engineers began to concern themselves with the problems associated with fluctuating loads in bridges, marine equipment, and power generation machines. By 1900, over 80 papers had been published on the subject of fatigue failures. During the first part of the twentieth century, more effort was placed on understanding the mechanisms of the fatigue process rather than just observing its results. This activity finally led, in the late 1950s and early 1960s, to the development of two approaches to fatigue life estimation. One method, known as the Manson-Coffin local strain approach, attempts to describe and predict crack initiation whilst another is based on linear elastic fracture mechanics, LEFM, and was developed to explain crack growth. Most recently, Miller and his colleagues at Sheffield University, England, have been working on ways of finding a unified theory of metal fatigue, describing crack growth on a microscopic, macroscopic, and structural level.

From this vast wealth of knowledge, one thing has become clear; modern design analysts and engineers will not create more fatigue resistant components and structures by indulging in more experimentation, although the need for more research is ever present. From a practical point of view, a more profitable approach is the implementation and efficient use of the knowledge which is available today.

2.2. Basic Factors of Fatigue Failure

Fatigue failure is a progressive, localised and permanent damage which appears in those parts under fluctuating stresses and strains. Above certain stress levels, fatigue gives rise to cracks or fractures after a

sufficient number of cycles have elapsed. It can be considered as a combination of cyclic stress, tensile stress and strains and, if any of those factors is absent, fatigue failure will not initiate or propagate. Many fatigue cracks are initiated and grow from structural defects, so that the theoretical fatigue life is reduced.

There are three common ways in which stresses may be applied: axial, torsional, and flexural [3].

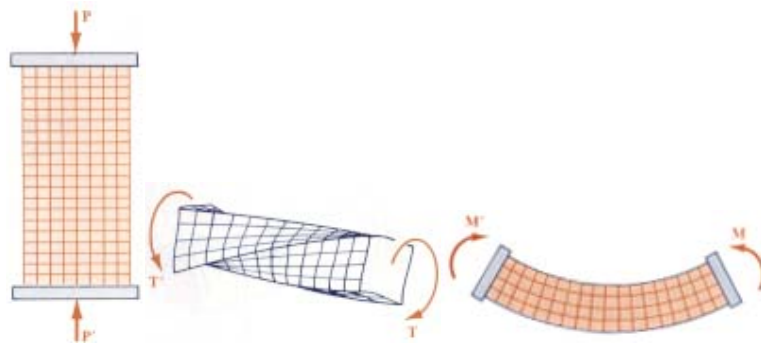


Figure 2.1 Axial, Torsional and Flexural Stresses [3]

There are also three stress cycles with which loads may be applied to the sample. The simplest being the reversed stress cycle. This is merely a sine wave where the maximum stress and minimum stress differ by a negative sign. An example of this type of stress cycle would be in an axle, where every half turn or half period as in the case of the sine wave, the stress on a point would be reversed. The most common type of cycle found in engineering applications is where the maximum stress (σ_{max}) and minimum stress (σ_{min}) are asymmetric (the curve is a sine wave) not equal and opposite. This type of stress cycle is called repeated stress cycle. A final type of cycle mode is where stress and frequency vary randomly. An example of this would be automobile shocks, where the frequency

magnitude of imperfections in the road will produce varying minimum and maximum stresses.

2.3. Fatigue Life

Fatigue life can be defined as the number of stress cycles required to cause failure; being a function of many variables; stress level, cyclic wave form, metallurgical condition of the material, manufacturing processes etc. This wide range of variables makes analytical prediction of fatigue failure difficult. Many repeated tests on similar components in service has been shown as the only available procedure. Laboratory tests, however, are essential in understanding fatigue behavior.

2.3.1. Factors Affecting Fatigue Life

- Mean stress (lower fatigue life with increasing σ_{mean}).
- Surface defects (scratches, sharp transitions and edges). Solution:
 - polish to remove machining flaws
- Add residual compressive stress (e.g., by shot peening.)
- Case harden, by carburizing, nitriding (exposing to appropriate gas at high temperature)
- Thermal cycling causes expansion and contraction, hence thermal stress, if component is restrained. Solution:
 - eliminate restraint by design
 - use materials with low thermal expansion coefficients.
- Corrosion fatigue. Chemical reactions induced pits which act as stress raisers. Corrosion also enhances crack propagation. Solution:
 - decrease corrosiveness of medium, if possible.
 - add protective surface coating.
 - add residual compressive stresses.

2.3.1.1. Effects of Material Condition on Fatigue

Localised plastic deformation is responsible for crack propagation, and microstructure of the material can affect crack growth, either inhibiting or modifying it. Some metal conditions which affect fatigue are:

Alloying: The influence of chemical composition on fatigue is approximately proportional to its influence on tensile strength.

Second phases: These affect crack propagation due to the strain caused by the presence of the second phase, the stress concentration of the second phase (shape, distribution) and the nature of the bond.

Work hardening: Work-hardened alloys show lower crack propagation rates and small deformation increases during fatigue. Fatigue strength can be increased by cold working.

Heat Treatment: Fatigue strength is generally increased by any heat treatment that increases tensile strength.

2.3.1.2. Effects of Manufacturing Practices on Fatigue

Manufacturing practices influence fatigue performance by affecting the intrinsic fatigue strength of material near the surface, by introducing or removing residual stress in the surface layers, and by introducing or removing irregularities on the surface that act as stress raisers.

Machining: Heavy cuts, residual marks, etc can promote fatigue failure.

Drilling: The fatigue strength of components can be reduced merely by the presence of a drilled hole.

Grinding: Proper grinding practice produces a smooth surface that is essentially free of induced residual stresses or sites for the nucleation of fatigue cracks. However, abusive grinding is a common cause of reduced fatigue strength

Surface compression: Compressive residual stress increase fatigue life. This can be obtained by shot peening, producing visible marks on the surface, such as dimples.

Plating: Electroplating can impair the fatigue strength by virtue of hydrogen embrittlement.

Cleaning: Some alkaline solutions are not satisfactory because they attack the surface.

Welding Practices: Can have an effect on the fatigue strength of a metal at and below the surface.

Identification marks: High stresses may be introduced into components by identification marks (date, part number, etc).

2.4. The S-N Curve

A very useful way to visualize time to failure for a specific material is with the S-N curve. The "S-N" means stress versus cycles to failure, which when plotted uses the stress amplitude, σ_a plotted on the vertical axis and the logarithm of the number of cycles to failure [4]. An important characteristic to this plot as seen in Fig. 2.2 is the fatigue limit.

The significance of the fatigue limit is that if the material is loaded below this stress, then it will not fail, regardless of the number of times it is loaded. Material such as aluminum, copper and magnesium do not show a fatigue limit, therefore they will fail at any stress and number of cycles.

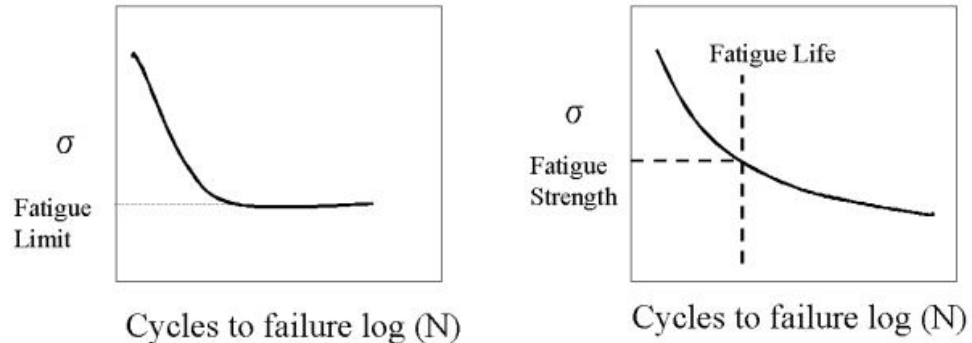


Figure 2.2 Typical S-N Curves [4]

Other important terms are fatigue strength and fatigue life. The stress at which failure occurs for a given number of cycles is the fatigue strength. The number of cycles required for a material to fail at a certain stress is fatigue life.

2.5. Gun Barrel Fatigue Process

a. Heat checks

- (1) Also known as crack initiations.
- (2) Small (sometimes invisible to the naked eye) cracks in the surface of the bore.
- (3) Can reach an approximate depth of .005" to .025".
- (4) May also start to occur after firing approximately 300 rounds.

b. Slow crack growth

- (1) Once the heat checks/cracks are formed, these cracks continue to grow slowly under the influence of stress in the gun barrel wall arising from the pressure versus time history during firing.
- (2) At this stage the heat check/crack will appear in a checking pattern and will be deeper than .025".
- (3) Heat checks/cracks will then connect together to form longitudinal and circumferential cracks.
- (4) Longitudinal cracks which are long and continuous and reach a length of approximately 2.5" to 3" will result in the condemning of the gun barrel.
- (5) Circumferential cracks which extend approximately one of third the inside circumference of the gun barrel are justification for condemning the gun barrel.

c. Fast crack fracture

- (1) When the crack grows at a very rapid rate (which can reach 5000 ft per sec) a condition known as fast fracture is reached. This condition produces catastrophic failure of the gun barrel structure

d. Gas washes

- (1) Also known as flame washes
- (2) Generally occur near the origin of the bore
- (3) Steel in the barrel physically melts away.
- (4) Caused by hot high velocity gases

e. Gas pockets

- (1) Concentrated area of gas washes
- (2) Melting of the gun barrel interior surface causing imperfections
- (3) Gas pockets which obtain a depth of .100" constitute criteria for regunning.

2.6. Effect Of Temperature On Fatigue Failure

For most metals, failure by fatigue can occur at any temperature below the melting point and the characteristic features of fatigue fractures, usually with little or no deformation, are apparent over the whole temperature range. The results of the fatigue tests show a similar stress-endurance relation at all temperatures, although at high temperatures there is seldom a fatigue limit and the downward slope of the curve is usually steeper than at air temperature. At high temperatures, the limiting factor in design is usually static strength, but resistance to fatigue is an important consideration in engine design, particularly when static and alternating stresses are combined. In addition, many service failures occur by thermal fatigue resulting from repeated thermal expansion and contraction [5].

The fatigue behaviour of a carbon steel is that they show a fatigue limit at room temperature but this disappears at high temperatures. The relation of the fatigue strength to the temperature is unusual, the fatigue strength increasing to a maximum value at a temperature of about 350⁰C-400⁰C. It is suggested that both the presence of a fatigue limit and a peak in the fatigue strength-temperature curve may be attributed to strain aging.

During low cycle fatigue operations, above 350°C – 400°C surface oxide cracks are formed. They act as oxide filled wedges and penetrate transgranularly [12].

2.6.1. The Stress-Endurance Curve At Different Temperatures

At high temperatures the stress - endurance curve for steels does not show a sharp limit, as it does at room temperature. Instead, the curve has a continuous downward trend beyond 10^8 cycles (fig. 2.3). Fatigue strengths at high temperatures must therefore be quoted, not as fatigue limits, but as stress ranges that can be withstood for a certain number of stress cycles without fracture [6].

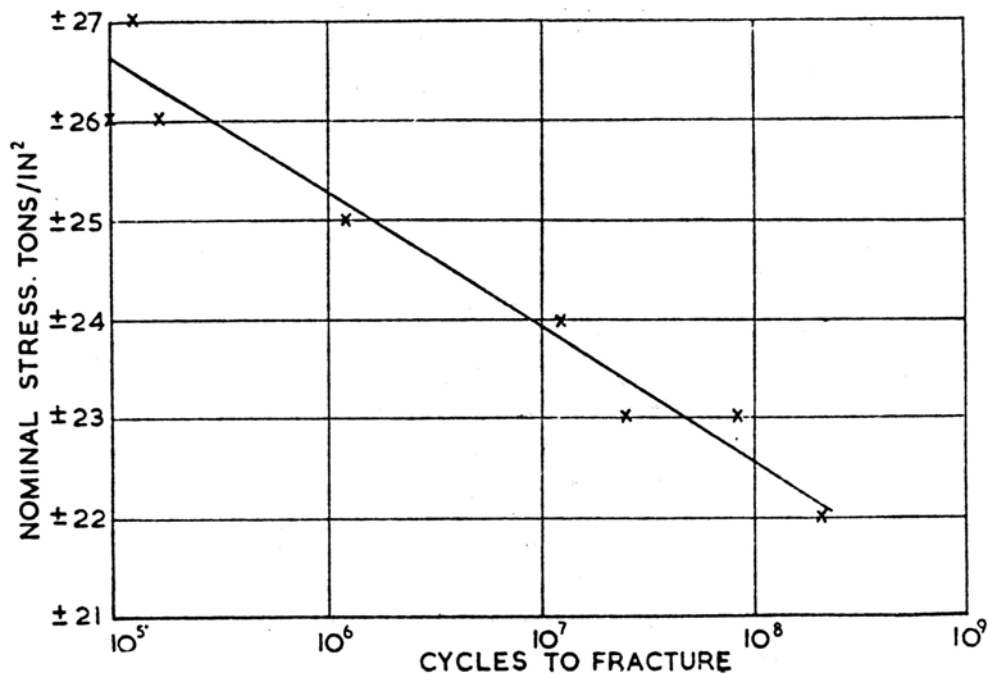


Figure 2.3 High Temperature S-N Curve for 0.17% C Steel at 400°C [6]

It is interesting to consider the significance of the fatigue limit. It has been suggested that the lack of a fatigue limit in steels at high temperatures might be attributed to corrosion. In other words, that failure occurs by corrosion fatigue in air.

The presence of a fatigue limit suggests that some strengthening process is coming into play after about 10^6 cycles, which more than counter-balances the damaging process. Thus, the fatigue strength of those materials with a fatigue limit can be increased by understressing (cyclic stressing at or below the fatigue limit) and by rest periods, while others cannot. This strengthening process is unlikely to be work-hardening, since many metals which show considerable capacity for work-hardening, e.g. copper, do not show a fatigue limit. The understressing effect is governed by a strain-aging process and it seems possible that the fatigue limit may also be attributed to strain aging.

2.6.2. The Fatigue Strength Of Steels At High Temperatures And Comparison With Other Mechanical Properties

A comparison of fatigue strengths at high temperatures with other mechanical properties shows that, as at room temperature, the fatigue strength is quite closely related to the tensile strength, unless the temperature is so high that the tensile strength is appreciably affected by creep.

Carbon steels show an unusual fatigue behaviour at high temperature. From a minimum value at about 100°C , the fatigue strength increases with increase in temperature by as much as 40% to a maximum value at about 350°C - 400°C , then, with further increase in temperature, decreases rapidly [5]. Above 400°C the creep strength falls off much more rapidly than the fatigue strength and much more attention has therefore been paid to creep strengths than to high temperature fatigue strengths. Alloy steels for use at high temperatures have been developed primarily to withstand creep. In general, those steels with high creep strengths also

have high fatigue strengths at high temperatures. For this purpose, it is found that the most effective alloying element is molybdenum, and further improvement is achieved by small additions of chromium or vanadium. Alloys of this type retain appreciable fatigue strength up to 600°C.

The strengths of quenched and tempered alloy steels decrease rapidly as the service temperature approaches the tempering temperature. For service above 400°C to 450°C, it is usually found that steels in the normalized or normalized and tempered conditions have a superior creep resistance, although at lower temperatures they are inferior to quenched and tempered steels.

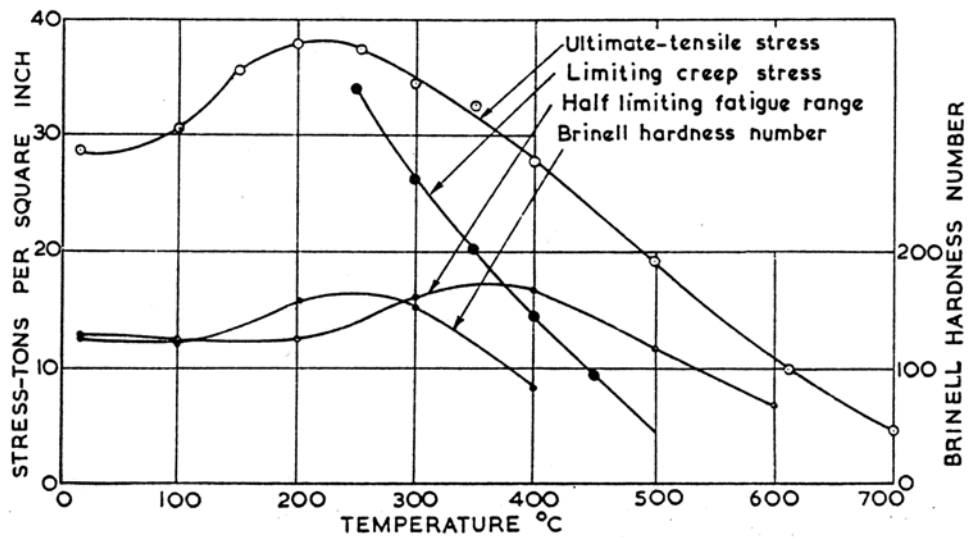


Figure 2.4 High Temperature Mechanical Properties for 0.17% C Steel at 400°C [6]

The static tensile strength also shows an increase with increase in temperature, but of smaller magnitude, with a maximum strength at about 200°C-250°C (fig. 2.4). This behaviour is attributed to the strengthening

effect of strain aging. The fatigue behaviour is also influenced by the strain ageing process, the peak occurring at a higher temperature because of the higher rate of strain imposed in the fatigue tests. Cast iron behaves in a similar manner, but the effect is smaller or absent in alloy steels. At room temperature, a rough working rule gives the fatigue strength of steels equal to half the tensile strength. As the fatigue behaviour differs from the tensile behaviour with increasing temperature, this rule does not hold at high temperatures. Thus, for the 17%C steel the ratio is 0.44 at room temperature falls to 0.33 at 200⁰C and rises to 0.6 at 400⁰C.

2.6.3. Effect Of Testing Frequency

At room temperature the frequency has little effect on the fatigue strength of most metals (except at very high frequencies), although a reduction in frequency may reduce slightly the number of cycles to failure at a given stress range.

The effect usually becomes greater with increase in the temperature, so that failure tends towards dependence on the total time of application of the stress range instead of on the number of cycles. This behaviour probably arises because at low temperatures deformation occurs almost immediately a stress is applied, whereas at high temperatures deformation continues under stress.

Some recent experiments on a 0.17%C steel showed that at temperatures between 400⁰C and 500⁰C the fatigue strength depended on the time to failure and was approximately independent of the speed [6]. This behaviour can be markedly influenced by metallurgical changes in the material.

The metallurgical change in this instance is strain ageing. At the lower frequency there is more time during the course of a stress cycle for ageing to occur, so that the maximum benefit is obtained at a lower temperature.

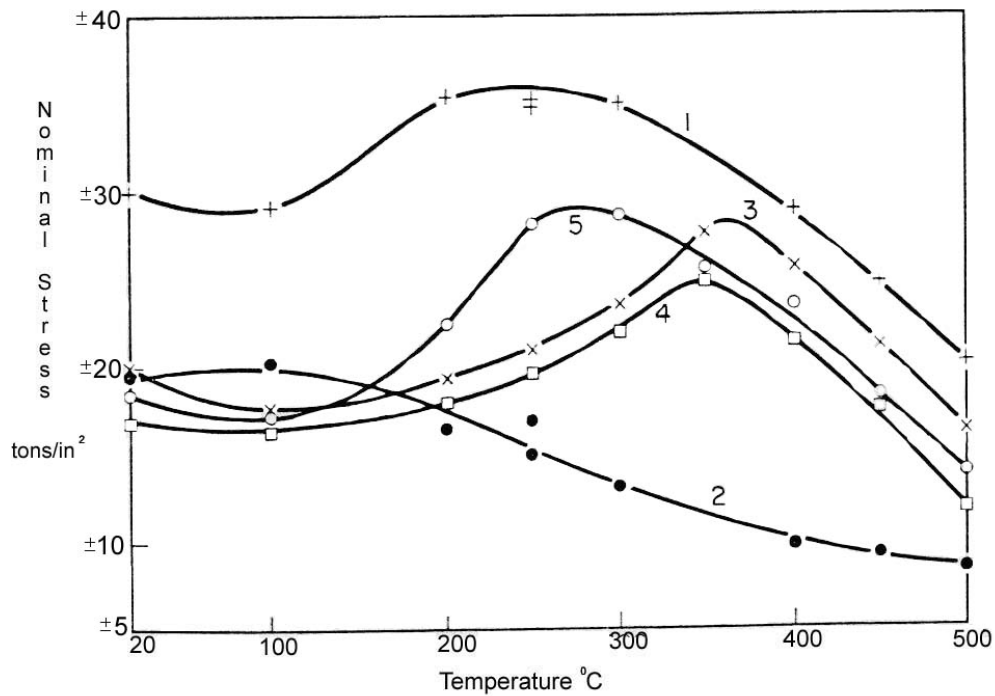


Figure 2.5 Frequency Effect on Fatigue Life of 0.17% C Steel at 400°C _1. Tensile Strength 2. Yield Point 3. Fatigue for 500000 cycles (2000 cycles/min) 4. Fatigue for 10⁸ cycles (2000 cycles/min) 5. Fatigue for 500000 cycles (10 cycles/min) [5]

2.6.4. Effect Of Metallographic Structure

At moderate temperatures a fine grain-size gives a higher creep resistance than a coarse grain-size, but this is reversed at high temperatures, because the grain boundaries becomes weaker than the grains. At moderate temperatures the fractured surfaces are appeared to be transgranular, whereas at high temperatures they are intergranular. The fatigue strength is also influenced in a similar manner, but the change from transgranular to intergranular fracture occurs at higher temperatures. Consequently, there is a range of temperature, which is often one that is important practically, when a coarse grain-size produces higher creep

strength, but lower fatigue strength. It is possible that better fatigue strengths would be achieved by under-ageing treatments [5].

The high-temperature fatigue strengths of castings are nearly always lower than those of forged alloys of similar composition. In this respect the fatigue behaviour differs from creep, for the creep strength of castings is often superior to forgings when the temperature is very high. One of the reasons for this is that the grain size is often greater in cast materials and if care is taken to produce fine-grained castings the fatigue strengths are improved.

The size of dislocation cells is dependent on test temperature, decreasing up to a certain limit and then increasing. This decrease in cell size indicates an increase in total dislocation density. As cell size decreases, rapid dislocation multiplication and rapid locking of mobile dislocations occur.

Fatigue life changes with grain size and temperature as shown in figure 2.6 [7].

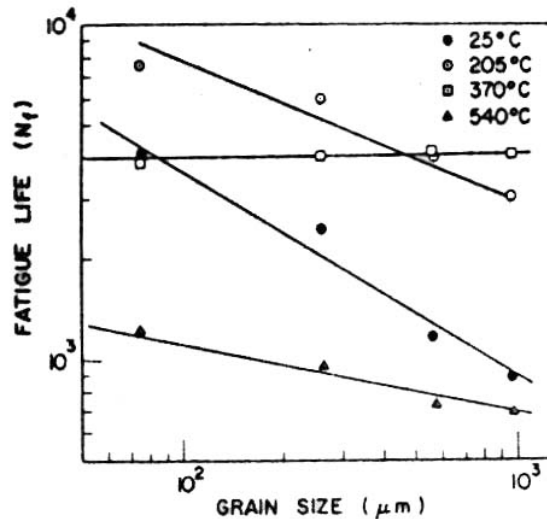


Figure 2.6 Effect of Grain Size at Ferrovac Iron [7]

Fatigue life (N_f) can be expressed in terms of grain size (D) at constant temperature by the relation:

$$N_f = aD^b \quad (2.1)$$

where a and b are constants.

The parameters a and b which determine the dependency of fatigue life on grain size and temperature may be considered also as parameters describing the dependency of crack propagation rate on these variables. These parameters are highly dependent on the fracture mechanism and its interaction with grain boundaries. Dynamic strain ageing induces changes in cyclic deformation characteristics and the fracture mechanism. The interaction of the fracture process with grain boundaries determines the degree of fatigue life dependency on grain size. Grain boundaries act as obstacles to this fracture process. Consequently, an increase in grain size decreases resistance to the fracture process, resulting in a higher crack growth rate and decreased life.

Thus, the fatigue life dependency on grain size and temperature can be explained in terms of the dynamic strain ageing potential.

2.6.5. Effect Of Plastic Deformation During Fatigue

Recent experiments done on mild steels show that at room temperature the material at the beginning of the test is deforming elastically, but an increasing plastic strain per cycle develops during the test. This shows that fatigue stressing causes a work softening and not a work hardening.

At 400⁰C-500⁰C the mild steel shows less plastic deformation during fatigue than at room temperature [6].

The results at 400⁰C indicate a progressive work-hardening until no measurable plastic strain occurs and this condition is followed by fracture (fig. 2.7). This shows that mild steel shows less crackless plasticity at high temperatures than at room temperatures.

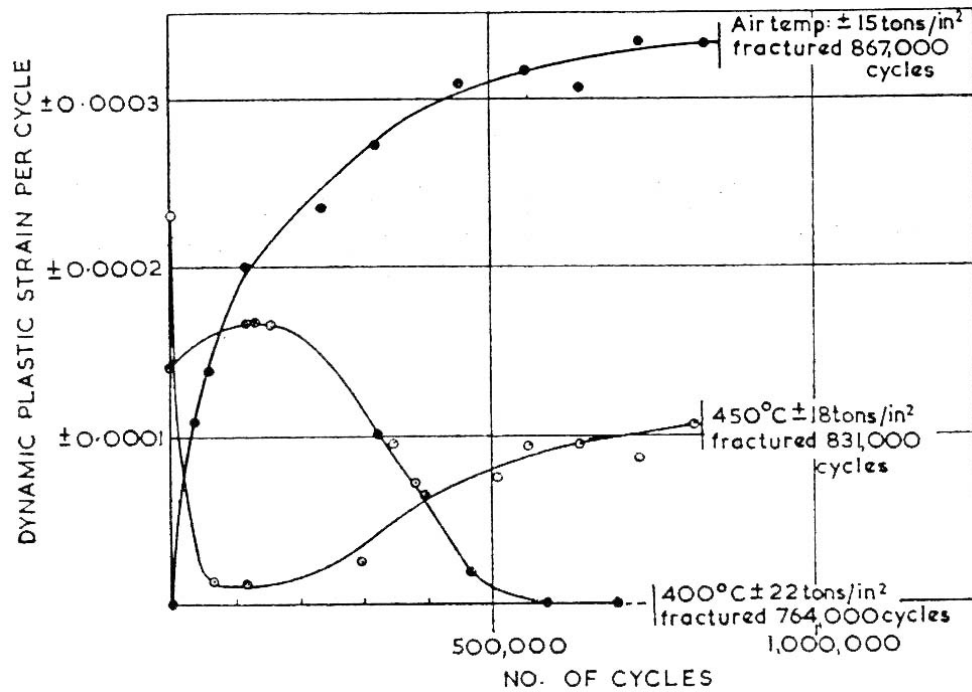


Figure 2.7 Effect of Plastic Deformation at Mild Steels [6]

2.7. Fatigue Crack Propagation

Failure problems which result from fatigue generally follow three phases:

Phase I - Initiation: Fatigue failure leads to crack nucleation and crack propagation. This initial phase never extends over more than five grains around the origin. Sometimes phase I may not be discernible, depending on material, environment, etc.

Phase II - Propagation: Progressive cyclic growth of a crack until the remaining uncracked cross section becomes too weak to sustain the loads imposed.

Phase III - Fracture: Remaining cross section suddenly fractures as a result of the loads imposed.

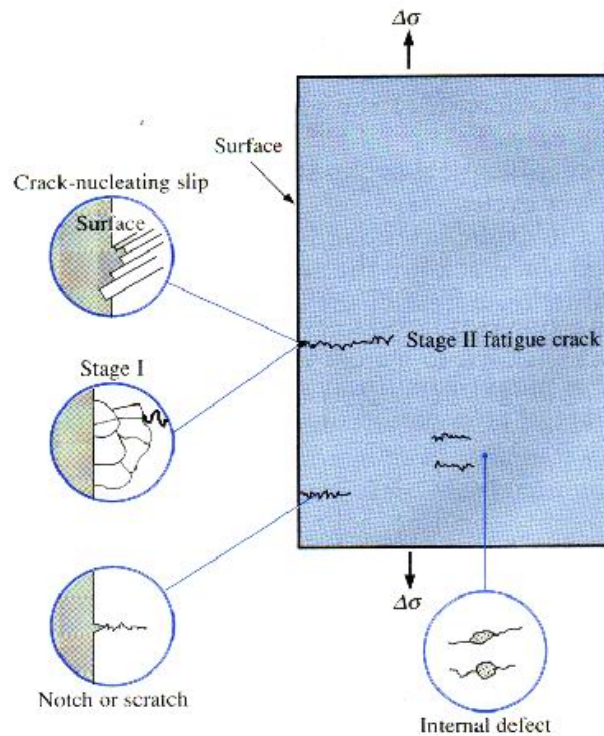


Figure 2.8 Phases of Fatigue Failure [4]

The fatigue life N_f , is the total number of cycles to failure, therefore can be taken as the sum of the number of cycles for crack initiation N_i and crack propagation N_p :

$$N_f = N_i + N_p \quad (2.2)$$

The contribution of the final phase to the total fatigue life is insignificant since it occurs so rapidly. Cracks associated with fatigue failure almost always initiate or nucleate on the surface of a component at some point of stress concentration. Crack nucleation sites include surface scratches, sharp fillets, and keyways [4].

Once a stable crack has nucleated, it then initially propagates very slowly and, this is sometimes called *stage I propagation*. This stage may constitute a large or small fraction of the total fatigue life depending on

stress level and the nature of the test specimen; high stress and the presence of notches favor a short-lived phase I.

Eventually, a second propagation stage (phase II) takes over, wherein the crack extension rate increases dramatically. Furthermore, at this point there is also a change in propagation direction to one that is roughly perpendicular to the applied tensile stress. During this stage of propagation, crack growth proceeds by a repetitive plastic blunting and sharpening process at the crack tip.

The region of a fracture surface that formed during phase II propagation may be characterized by two types of markings termed *beachmarks* and *striations* (fig. 2.9).

Both of these features indicate the position of the crack tip at some point in time and appear as concentric ridges that expand away from crack initiation sites, frequently in a circular or semicircular pattern. Beachmarks are of macroscopic dimensions, and may be observed with an unaided eye (fig. 2.10).

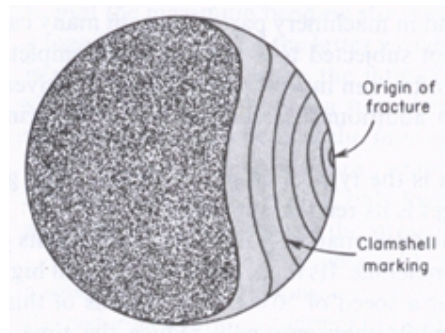


Figure 2.9 Beachmarks or “Clamshell Pattern” [4]

On the other hand, fatigue striations are microscopic in size and subject to observation with the electron microscope either with TEM or SEM.



Figure 2.10 Example of the Striations Found in Fatigue Fracture [4]

Striation width depends on, and increases with, increasing stress range. It must be emphasized that although both beachmarks and striations are fatigue fracture surface features having similar appearances, they are nevertheless different, both in origin and size. There may be literally thousands of striations within a single beachmark.

Beachmarks and striations will not appear on that region over which the rapid failure occurs. Rather, the rapid failure may be either ductile or brittle, failure.

2.7.1. Influence Of Temperature On Fatigue Crack Propagation

The basic process of fatigue failure in metals at ambient temperature is the relatively rapid nucleation of small surface cracks followed by the steady slow growth of one or more of these cracks until material separation occurs, or the crack achieves a critical size for fast

fracture [8]. At elevated temperatures, although this process persists as the dominant one, secondary effects are observed which can particularly influence the rate of crack growth. Such effects include the weakening of grain boundaries, the development of internal grain boundary cracks or cavities, and an enhanced rate of oxidation of freshly exposed fracture surfaces. The relative weakness of grain boundaries induces a change of crack path from predominantly transgranular to intergranular at high temperatures and low rates of straining.

2.7.2. Fatigue Crack Propagation Rate

Under the influence of cyclic stresses, cracks will inevitably form and grow; this process, if unabated, can ultimately lead to failure. The rate at which a crack grows has considerable importance in determining the life of a material. The propagation of a crack occurs during the second step of fatigue failure. As a crack begins to propagate, the size of the crack also begins to grow. The rate at which the crack continues to grow depends on the stress level applied. [3] The rate at which a crack grows can be seen mathematically in equation 2.3 by:

$$\frac{da}{dN} = A(\Delta K)^m \quad (2.3)$$

The variables A and m are properties of the material, da is the change in crack length, and dN is the change in the number of cycles. K is the change in the stress intensity factor or by equation 2.4:

$$\Delta K = K_{\max} - K_{\min} = Y\Delta\sigma\sqrt{\pi a} \quad (2.4)$$

Rearrangement and integration of Eq. 1 gives us the relation of the number of cycles of failure, N_f , to the size of the initial flaw length, a_o , and the critical crack length, a_c , and Eq. 2:

$$N_f = \int_0^{N_f} dN = \int_{a_o}^{a_c} \frac{da}{A(Y\Delta\sigma\sqrt{\pi a})^m} = \frac{1}{A\pi^{m/2}(\Delta\sigma)^m} \int_{a_o}^{a_c} \frac{da}{Y^m a^{m/2}} \quad (2.5)$$

2.8. High Cycle versus Low Cycle Fatigue

Over the years, fatigue failure investigations have led to the observation that the fatigue process actually embraces two domains of cyclic stressing or straining that are distinctly different in character. In each of these domains, failure occurs by apparently different physical mechanisms: one where significant plastic straining occurs and the other where stresses and strains are largely confined to the elastic region. The first domain involves some large cycles, relatively short lives and is usually referred to as low-cycle fatigue. The other domain is associated with low loads and long lives and is commonly referred to as high-cycle fatigue. Low-cycle fatigue is typically associated with fatigue lives between about 10 to 100,000 cycles and high-cycle fatigue with lives greater than 100,000 cycles.

In the high-cycle fatigue domain, measures such as shot peening and other surface hardening treatments or the use of higher strength materials are beneficial. For low-cycle fatigue, where ductility and resistance to plastic flow are important, these measures are inappropriate.

2.8.1. Low Cycle (Cyclic Strain-Controlled) Fatigue

2.8.1.1. Cycle-Dependent Material Response

Cycle-dependent material response under stress and strain control are shown in Figs. 2.11 and 2.12, respectively, which reflect changes in the shape of the hysteresis loop [1].

It is seen that, in both cases, the material response changes with continued cycling until cyclic stability is reached. That is, the material becomes either more or less resistant to the applied stress and strains. Therefore, the material is said to cyclically strain harden or strain soften. Referring to Fig. 2.13 for the case of stress control, where the fatigue test is conducted in a stress range between P' and S' , the width of the hysteresis loop TQ (the plastic strain range) contracts when cyclic hardening occurs and expands during cyclic softening.

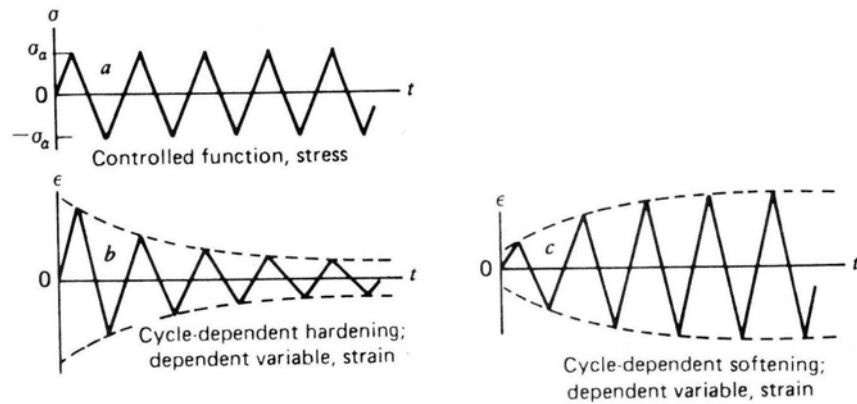


Figure 2.11 Cycle-dependent material response under stress control [1]

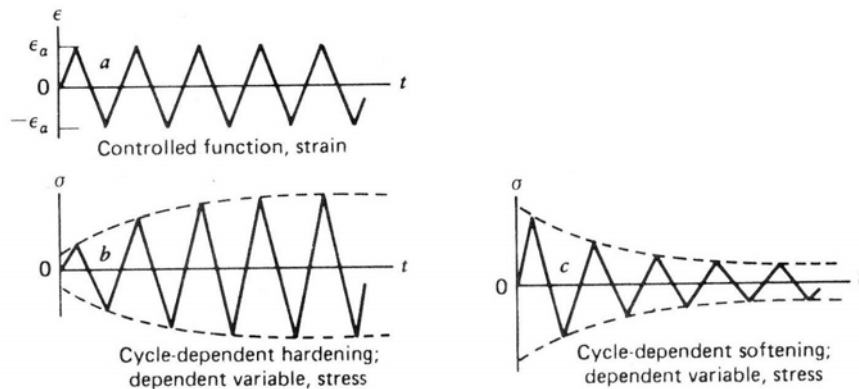


Figure 2.12 Cycle-dependent material response under strain control [1]

Cyclic softening under stress control is a particularly severe condition because the constant stress range produces a continually increasing strain range response, leading to early fracture (Fig. 2.11). Under cyclic strain conditions within limits of strains X and Y, hysteresis loop expands above P and below S for cyclic hardening and shrinks below P and above S for cyclic softening.

Manson et al. observed that the propensity for cyclic hardening or softening depends on the ratio of monotonic ultimate strength to 0.2%

offset yield strength. When $\sigma_{ult}/\sigma_{ys} > 1.4$, the material will harden, but when $\sigma_{ult}/\sigma_{ys} < 1.2$, softening will occur. For ratios between 1.2 and 1.4, forecasting becomes difficult, though a large change in properties is not expected. Also if $n > 0.20$, the material is likely to strain harden, and softening will occur if $n < 0.10$. Therefore, initially hard and strong materials will generally cyclically strain soften, and initially soft materials will harden.

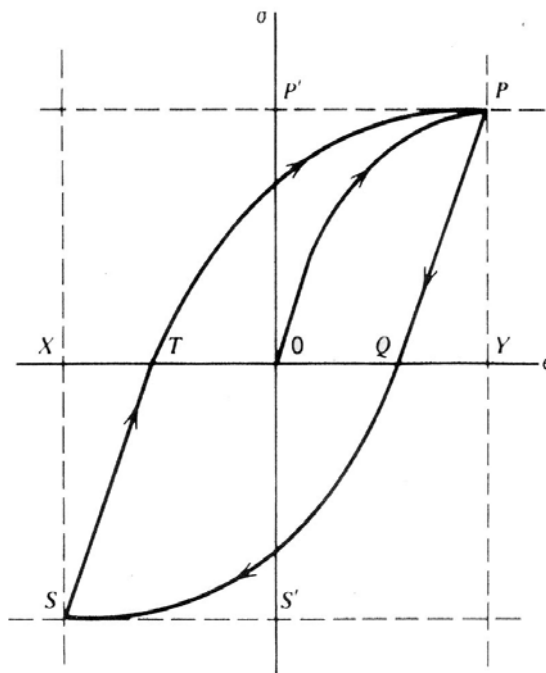


Figure 2.13 Hysteresis Loop [1]

The answer to the question of which material cyclically harden or soften appears to be related to the nature and stability of the dislocation substructure of that material. For an initially soft material, the dislocation density is low. As a result of plastic strain cycling, the dislocation density increases rapidly, contributing to significant strain hardening. At some

point, the newly generated dislocations assume a stable configuration for that material and for the magnitude of cyclic strain imposed during the test. When a material is hard initially, subsequent strain cycling causes a rearrangement of dislocations into a new configuration that offers less resistance to deformation – that is, the material strain softens.

Dislocation mobility that strongly affects dislocation substructure stability depends on the material's stacking fault energy (SFE). When SFE is high, dislocation mobility is great because of enhanced cross-slip; conversely, cross-slip is restricted in low SFE materials. As a result, some materials cyclically harden or soften more completely than others.

If cyclic straining causes coarsening of a preexistent cell structure, then softening will occur. If the cell structure gets finer, then cyclic straining results in a hardening process.

2.8.1.2. Strain Life Curves

It is convenient to begin the analysis by considering the elastic and plastic strain components separately. The elastic component is often described in terms of a relation between the true stress amplitude and number of load reversals [9,10].

$$\Delta\epsilon_P = \Delta\epsilon_T - \frac{\Delta\sigma}{E} \quad (2.6)$$

$$\frac{\Delta\epsilon_e E}{2} = \sigma_a = \sigma_f' (2N_f)^b \quad (2.7)$$

where $\frac{\Delta\epsilon_e}{2}$ = elastic strain amplitude

E = modulus of elasticity

σ_a = stress amplitude

σ_f' = fatigue strength coefficient, defined by the stress intercept at one load reversal ($2N_f = 1$)

N_f = cycles to failure

b = fatigue strength exponent

Increased fatigue life is expected with a decreasing fatigue strength exponent b and an increasing fatigue strength coefficient σ_f' .

The plastic component of strain is best described by the Manson-Coffin relation:

$$\frac{\Delta\epsilon_p}{2} = \epsilon_f' (2N_f)^c \quad (2.8)$$

where $\frac{\Delta\epsilon_p}{2}$ = plastic strain amplitude

ϵ_f' = fatigue ductility coefficient, defined by the strain intercept at one load reversal ($2N_f = 1$)

$2N_f$ = total strain reversals to failure

c = fatigue ductility exponent, a material property.

Improved fatigue life is expected with a decreasing fatigue ductility exponent c and an increasing fatigue ductility coefficient ϵ_f' .

Manson et al. argued that the fatigue resistance of a material subjected to a given strain range could be estimated by superposition of the elastic and plastic strain components. Therefore, by combining Eqs. 2-6, 2-7, and 2-8, the total strain amplitude may be given by:

$$\frac{\Delta\epsilon_T}{2} = \frac{\Delta\epsilon_e}{2} + \frac{\Delta\epsilon_p}{2} = \frac{\sigma_f'}{E} (2N_f)^b + \Delta\epsilon_f' (2N_f)^c \quad (2.9)$$

The total strain life curve would approach the plastic strain life curve at large strain amplitudes and approach the elastic strain life curve at low total strain amplitudes. This is shown in Fig. 2.14 for a high-strength steel alloy.

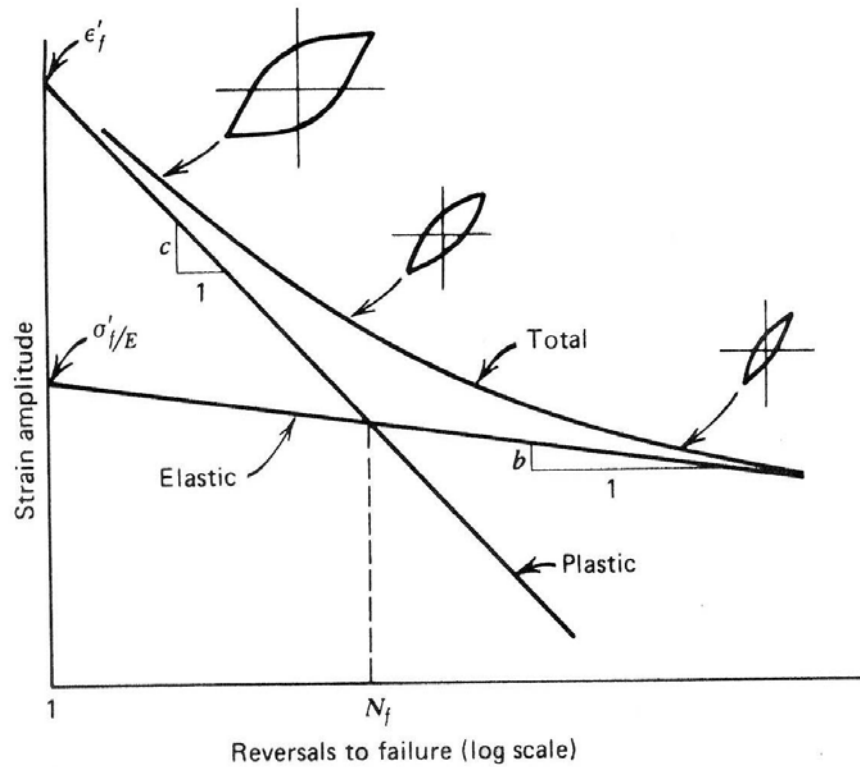


Figure 2.14 Strain-Life Curve [1]

2.8.1.3. Effect of Surface Treatment on Low Cycle Fatigue

For reasonably ductile metals in the low cycle fatigue region, the large amount of cyclic plastic strain which imposed during the fatigue test eliminates initial residual stress and greatly reduces the influence of small scratches and other stress raisers. Furthermore, at short lives where the slope of the strain-life curve is large, scatter results in small variation in life. When longer lives are expected and when metals have low ductility, the same care should be taken to obtain a smooth surface which is as free of residual stresses as is generally taken with long-life fatigue samples [9].

CHAPTER 3

EXPERIMENTAL PROCEDURE

3.1. Material

The material used in this study is DIN 35 NiCrMoV 12 5 gun barrel steel which has a similar composition with AISI/SAE 4340 steel. It was manufactured by ASİL ÇELİK – Bursa for Turkish Army Forces in order to be used as gun barrel production.

The microstructure of this steel is homogenous and consists of completely tempered martensite which is the result of conventional quenching and tempering (Figure 3.1).

It is a high strength low alloy steel (HSLA) processed with vacuum degassing technology. The chemical composition of the alloy in weight percentages is given in Table 3.1.

The tensile properties and fracture toughness values of AISI 4340 high strength low alloy steel are given in Tables 3.2 and 3.3 respectively. The hardness of the tested material is 33-35 Rockwell and UTS is found as 126 kg/mm². Tempering temperature is 540 – 550⁰C.

Table 3.1 Weight Percentages of Testing Material

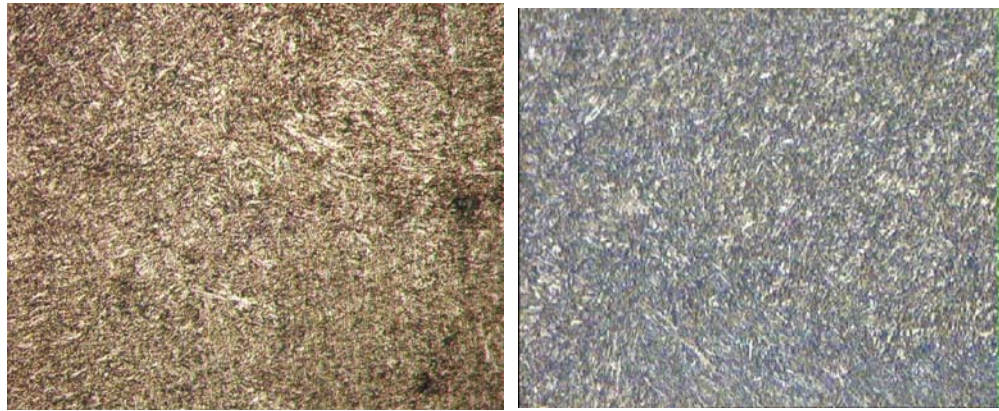
35 NiCrMoV 12 5	
Element	Weight Percentage (%)
C	0,3 – 0,4
Si	0,15 – 0,35
Mn	0,4 – 0,7
P	max. 0,015
S	max. 0,015
Cr	1,1 – 1,4
Mo	0,35 – 0,6
Ni	2,5 – 3,5
V	0,08 – 0,2
Al	max. 0,015
Fe	Balance

Table 3.2 Material Properties of AISI 4340 Steel [10]

Tempering Temperature (°C)	Tensile Strength (Mpa)	Yield Strength (Mpa)	Elongation (%)	Reduction in Area (%)	Hardness (Bhn)
216	1875	1675	10	38	520
327	1725	1585	10	40	486
438	1470	1365	10	44	430
549	1172	1075	13	51	360
660	965	855	19	60	280

Table 3.3 Fracture Toughness Value of Testing Material

Tempering Temperature (°C)	Fracture Toughness (N.mm^{-3/2})
540 – 550	4700 - 5100



(a) L-R direction

(b) R-L direction

Figure 3.1 Microstructure of As-Received DIN 35NiCrMoV125 Steel (50X)

3.2. Testing Specimen

All specimens were prepared according to ASTM E 606 – 92 [10]. The shape of the specimens is hour – glass type in order to obtain stress concentration in the middle of the specimen (the minimum diameter) (Fig. 3.2). At all tests, crack initiation and fracture occurred at the mid point of the specimens. Also, for each temperature, a tension test is done [11]. The results of tension tests are used to determine the maximum loads.

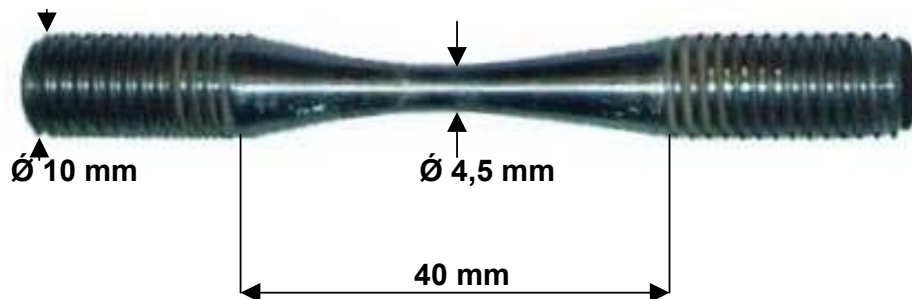


Figure 3.2 Dimensions of Testing Specimen

3.3. Fatigue Life Testing

All tests were performed on a closed – loop, servo – controlled hydraulically activated MTS 810 testing machine which has a 10 tons capacity. Specimens are machined along L direction. The orientation of the specimen is shown in figure 3.3.

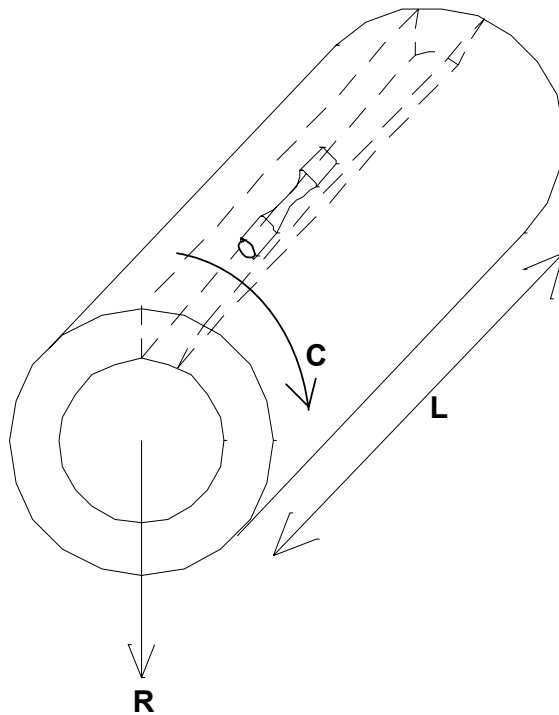


Figure 3.3 Orientation of Specimen

where;

L = Longitudinal

R = Radial

C = Circumferential

All tests were carried out at a frequency of 2 Hz. The type of the wave is haver sine (Fig. 3.4).

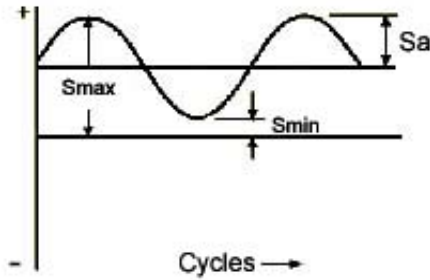


Figure 3.4 Haver Sine Wave

Three temperatures were used at this report (RT, 250⁰C, 400⁰C). The temperatures were chosen by considering the service life of that steel. Variables are chosen as temperature and load. Stress ratio, R, for all tests was 0,06. In low cycle testing, strain amplitudes between 0,2%-2% is used [9]. Maximum loads were determined from the tension tests that carried out for each temperature (tables 3.4, 3.6, 3.8). The maximum - minimum stresses and stress amplitudes applied for each temperature are listed in tables 3.5, 3.7, and 3.9. Duplicates of each experiment are done in order to obtain more accurate results.

Table 3.4 Room Temperature Strain and Load Values

Room Temperature Strain and Load Values					
d₀=4,5 (mm)	0,2%strain	0,75%strain	1% strain	1,5%strain	2% strain
Load (kg)	1875	1915	1925	1950	1975
Stress(MPa)	1155	1181	1189	1204	1216

Table 3.5 Room Temperature S_{max} , S_{min} and S_a Values

Stress Max. (MPa)	Stress Min. (MPa)	Stress Amp. (MPa)
1216	72,96	571,52
1204	72,24	565,88
1189	71,34	558,83
1181	70,86	555,07
1155	69,30	542,85

Table 3.6 250⁰C Strain and Load Values

250 ⁰ C Strain and Load Values					
$d_0=4,5(\text{mm})$	0,2%strain	0,75%strain	1%strain	1,5%strain	2%strain
Load (kg)	1660	1715	1735	1760	1780
Stress(MPa)	1023	1056	1068	1086	1097

Table 3.7 250⁰C S_{max} , S_{min} and S_a Values

Stress Max. (MPa)	Stress Min. (MPa)	Stress Amp. (MPa)
1097	65,82	515,59
1086	65,16	510,42
1068	64,08	501,96
1056	63,36	496,32
1023	61,38	480,81

Table 3.8 400⁰C Strain and Load Values

400 ⁰ C Strain and Load Values					
$d_0=4,5(\text{mm})$	0,2%strain	0,75%strain	1%strain	1,5%strain	2%strain
Load (kg)	1450	1525	1540	1555	1570
Stress(MPa)	894	941,5	950,5	958	961

Table 3.9 400°C S_{max}, S_{min} and S_a Values

Stress Max. (MPa)	Stress Min. (MPa)	Stress Amp. (MPa)
961	57,66	451,67
958	57,48	450,26
950,5	57,03	446,74
941,5	56,49	442,51
894	53,64	420,18

The furnace model is Satec Systems SF-15 Furnace. This furnace is of split construction hinged in the rear. The heating element provides three heat zones, and is wound for maximum continuous operation to 1200°C.

The three in I.D. of the furnace core permits either bar or sheet samples to be used. Quick disconnect latches with heat resistant handles keep furnace sections locked together during tests, and facilitate opening and closing the furnace. Closures at top and bottom of furnace fit snugly around pull-bars and reduce heat loss at these points. Max power required is 115 volts, single phase, 30 amperes, 60hz a.c. The heating range of the furnace is 0°C to 1200°C and it has a tolerance of ±5°C at every 600°C and ±1 for every additional 100°C.



Figure 3.5 Furnace Attached to MTS Testing Machine

For temperature measurement during the tests, a thermocouple is used. The position of the thermocouple is seen in the figure 3.6. Thermocouple were attached to the system by metallic wires and teflon bands.

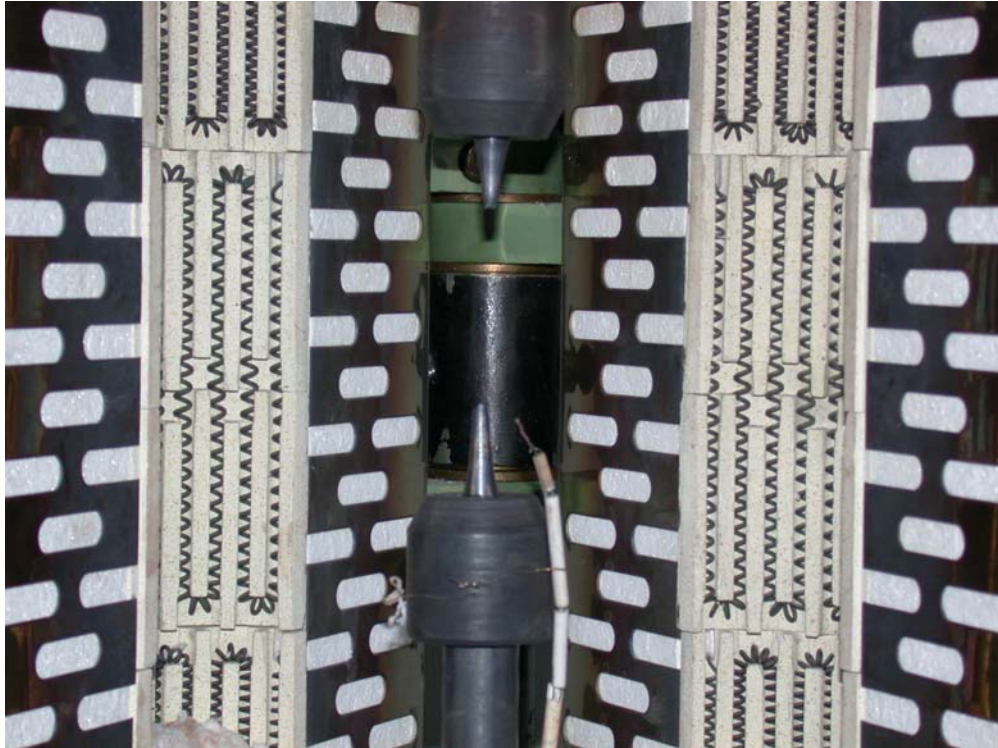


Figure 3.6 Position of Thermocouple

MTS testing machine, cylindrical extension of the furnace and the temperature controlling device are shown in figure 3.7.



Figure 3.7 The Whole Setup

3.4. Fractography

Fractographic analysis was used for macro and micro inspection of the fracture surfaces. To be able to observe the effect of the temperature and the strain difference on the specimens from macro and micro standpoint, both of the analysis were performed on the specimens chosen among the ones tested at three different testing temperatures and two different strains.

Macro analysis of the surface, by which the crack initiation sites are examined, was performed by a stereo optical microscope at a magnitude of 20X.

Through the micro fractography, examination of the fracture surfaces of all specimens for the typical indicators of fatigue fracture and sudden failure regions such as striations, primary cracks and secondary cracks, tear ridges and dimples, was possible. The study was done by JEOL – JSM 6400 Scanning Eletron Microscope (SEM) at an operation voltage of 20 kV.

CHAPTER 4

RESULTS AND DISCUSSIONS

As mentioned before, 5 to 10 experiments are needed to define the low cycle property of a material [9]. So, 5 different strain amplitudes were chosen. Also, for more accurate results, the duplicates of each experiment were done. Since the specimens are loaded at and above the yield strength, a large scatter in the results of duplicate experiments is not expected. 10 experiments at room temperature (RT), 10 experiments at 250⁰C and 10 experiments at 400⁰C, a total of 30 experiments, were seem to be enough for obtaining reasonable data. At each temperature, 5 different stress amplitudes were used. These stress amplitudes are the corresponding values of five chosen strain amplitudes. The strain amplitudes that were used are 2%, 1.5%, 1%, 0.75% and 0.2%. Corresponding values of these strain amplitudes were calculated from stress – strain diagrams obtained from the tension tests done at each temperature. Stress – strain diagrams for RT, 250⁰C and 400⁰C can be seen at figure 4.1. For all experiments stress ratio was 0.06 and frequency of testing was 2 cycles/sec.

4.1. Tension and Fatigue Test Results for RT, 250°C and 400°C

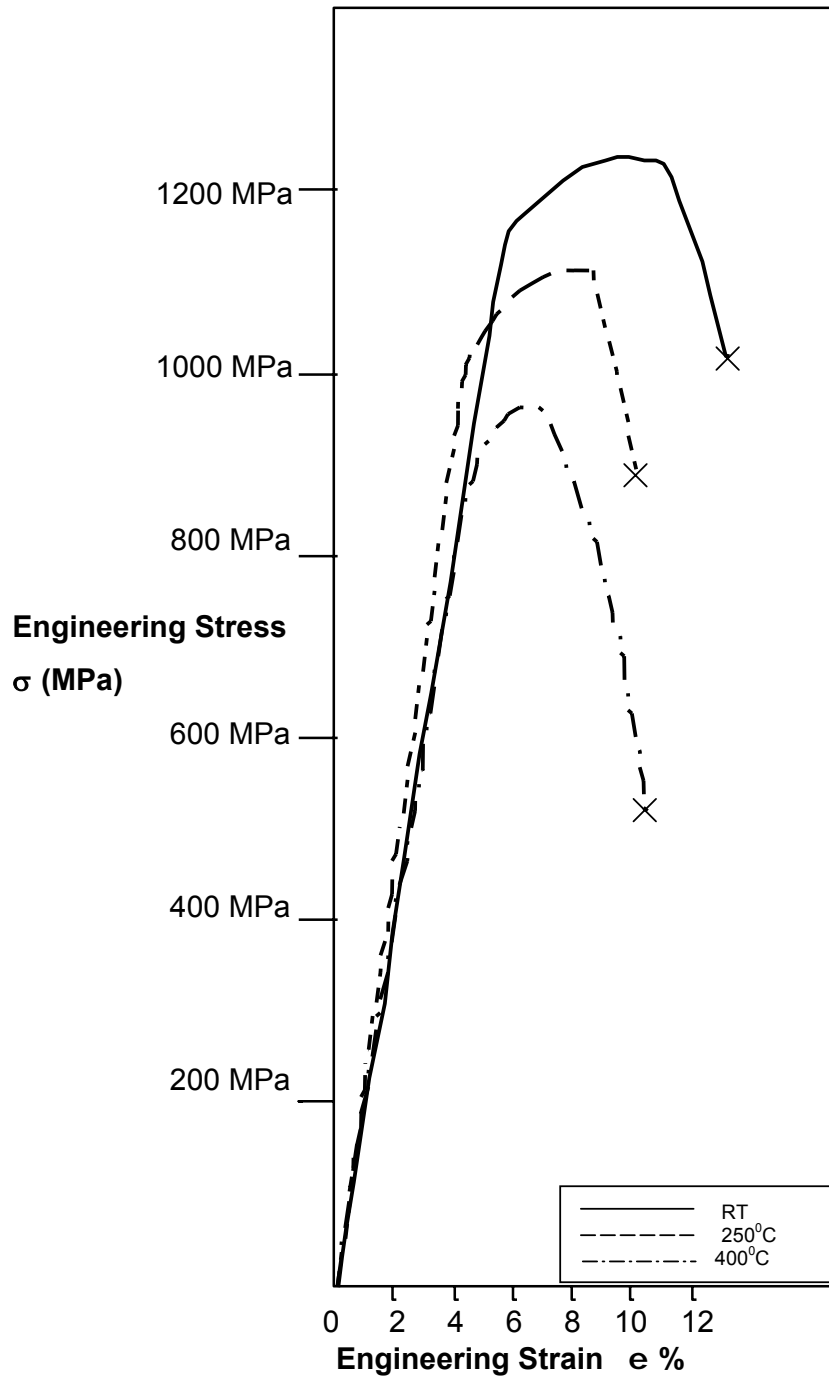


Figure 4.1 Engineering Stress (σ) versus Engineering Strain (e) diagrams for RT, 250°C and 400°C

Table 4.1 Room Temperature Mechanical Properties

Testing Temperature	Room Temperature
Yield Strength (MPa)	1155
UTS (MPa)	1239
Percent Elongation (%)	13.02
Reduction In Area (%)	45

Table 4.2 250⁰C Mechanical Properties

Testing Temperature (⁰C)	250 ⁰ C
Yield Strength (MPa)	1023
UTS (MPa)	1102
Percent Elongation (%)	10.15
Reduction In Area (%)	47

Table 4.3 400⁰C Mechanical Properties

Testing Temperature (⁰C)	400 ⁰ C
Yield Strength (MPa)	894
UTS (MPa)	981
Percent Elongation (%)	10.41
Reduction In Area (%)	70

Table 4.4 Room Temperature Fatigue Experiments

Room Temperature Fatigue Experiments				
Experiment No.	Minimum Stress (MPa)	Maximum Stress (MPa)	Stress Amplitude (MPa)	Total Cycle (N_f)
1	72,96	1216	571,52	4400
2	72,96	1216	571,52	5500
3	72,24	1204	565,88	5970
4	72,24	1204	565,88	7980
5	71,34	1189	558,83	10390
6	71,34	1189	558,83	10650
7	70,86	1181	555,07	12470
8	70,86	1181	555,07	19120
9	69,30	1155	542,85	31380
10	69,30	1155	542,85	36280

Table 4.5 250⁰C Fatigue Experiments

250⁰C Fatigue Experiments				
Experiment No.	Minimum Stress (MPa)	Maximum Stress (MPa)	Stress Amplitude (MPa)	Total Cycle (N_f)
1	65,82	1097	515,59	6050
2	65,82	1097	515,59	7600
3	65,16	1086	510,42	8060
4	65,16	1086	510,42	8550
5	64,08	1068	501,96	10400
6	64,08	1068	501,96	11630
7	63,36	1056	496,32	13950
8	63,36	1056	496,32	14940
9	61,38	1023	480,81	37860
10	61,38	1023	480,81	41500

Table 4.6 400°C Fatigue Experiments

400°C Fatigue Experiments				
Experiment No.	Minimum Stress (MPa)	Maximum Stress (MPa)	Stress Amplitude (MPa)	Total Cycle (N _f)
1	57,66	961	451,67	7500
2	57,66	961	451,67	9000
3	57,48	958	450,26	11000
4	57,48	958	450,26	13250
5	57,03	950,5	446,74	14750
6	57,03	950,5	446,74	16250
7	56,49	941,5	442,51	25000
8	56,49	941,5	442,51	27500
9	53,64	894	420,18	53750
10	53,64	894	420,18	55660

4.2. Fatigue Strength and Fatigue Ductility Curves

According to equations 2.7, 2.8 and 2.9, the low cycle fatigue (strain – life) curves have two components; one is elastic and the other is plastic.

The elastic component of these curves is defined as:

$$\sigma_a = \sigma_f' (2N_f)^b$$

This elastic component is defined as fatigue strength property curve and σ_f' value is the y – axis intercept of that curve.

Plastic component of strain – life curves is called as fatigue ductility curve which has the equation:

$$\frac{\Delta \epsilon_p}{2} = \epsilon_f' (2N_f)^c$$

where ϵ_f' is the y – axis intercept of that curve.

The combination of these equations gives the whole strain – life curve equation:

$$\frac{\Delta\epsilon_T}{2} = \frac{\Delta\epsilon_e}{2} + \frac{\Delta\epsilon_p}{2} = \frac{\sigma_f'}{E} (2N_f)^b + \Delta\epsilon_f' (2N_f)^c$$

The breakpoint of the strain – life curve, which is the transition point from elastic range to plastic range, corresponds to 1 % strain.

The values of fatigue strength coefficient, σ_f' , and fatigue strength exponent, b , are calculated by using the fatigue strength property curves (figure 4.2) and the equation 2.7. The values of fatigue ductility coefficient, ϵ_f' , and fatigue ductility exponent, c , are calculated by using the fatigue ductility property curves (figure 4.3) and the equation 2.8.

As there is no parameter in these equations which contains temperature as a variable, the effect of temperature to the shape of these curves is not expected.

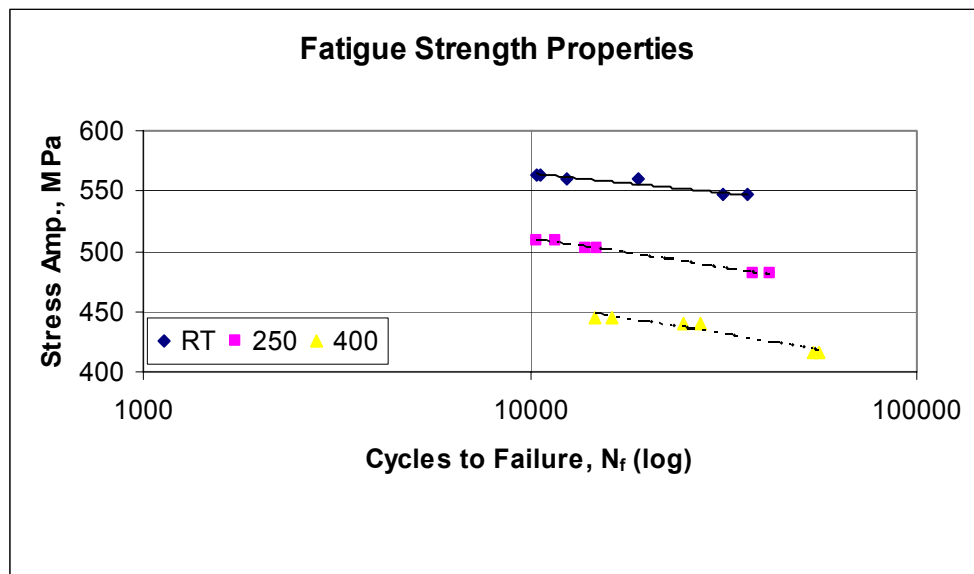


Figure 4.2 Fatigue Strength Properties

Fatigue Strength Coefficient_{RT} = σ_f' = 1446 MPa

Fatigue Strength Exponent_{RT} = b = - 0.026

Fatigue Strength Coefficient_{250C} = σ_f' = 1472 MPa

Fatigue Strength Exponent_{250C} = b = - 0.0433

Fatigue Strength Coefficient_{400C} = σ_f' = 1397 MPa

Fatigue Strength Exponent_{400C} = b = - 0.052

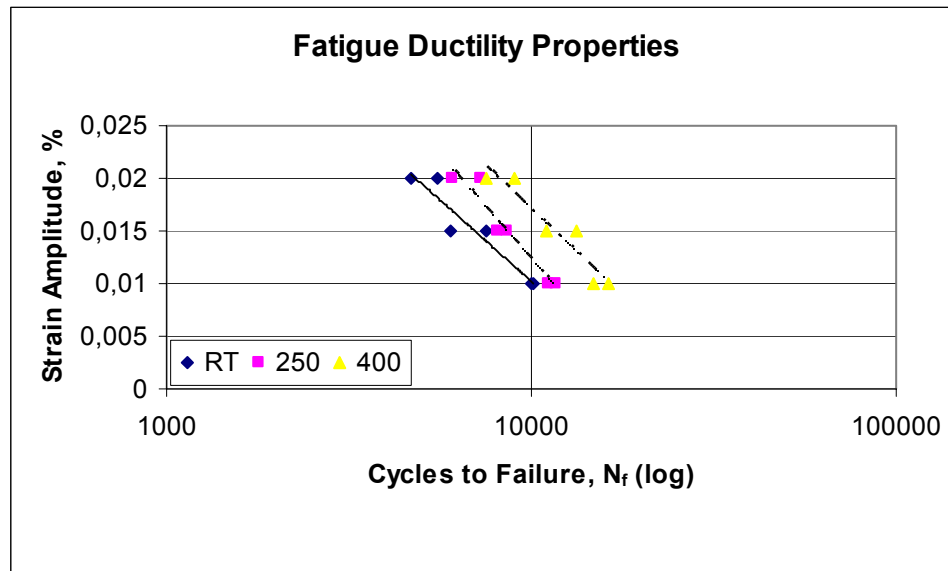


Figure 4.3 Fatigue Ductility Properties

Fatigue Ductility Coefficient_{RT} = ϵ_f' = 0.1191

Fatigue Ductility Exponent_{RT} = c = - 0.919

Fatigue Ductility Coefficient_{250C} = ϵ_f' = 0.1771

Fatigue Ductility Exponent_{250C} = c = - 1.448

Fatigue Ductility Coefficient_{400C} = ϵ_f' = 0.1478

Fatigue Ductility Exponent_{400C} = c = - 1.311

4.3. Elastic to Plastic Transition Life

In Figure 2.15, the point where the plastic and elastic life lines intersect is called the transition life. The transition life represents the point at which a stable hysteresis loop has equal elastic and plastic components. At lives less than the transition, plastic events dominate elastic ones and at lives longer than the transition elastic events dominate plastic ones. From this point of view, therefore, the transition life represents a very convenient and important way of delineating between the low- and high-cycle fatigue regimes.

This distinction is important because the solutions which may be proposed to a particular fatigue problem depend entirely on the dominant loading regime. Problems of high-cycle fatigue are usually tackled through the selection of stronger, higher UTS materials, or through the application of compressive surface stresses through shot peening or nitriding. These solutions would be largely ineffective for the treatment of a low-cycle fatigue problem. Indeed, the selection of a material with a higher UTS, and presumably a lower ductility, could well make the situation worse.

The experimental transition life results for the three temperatures can be determined from the figures 4.4, 4.5 and 4.6. From these figures, it can be seen that at 0.1 % strain amplitude the slope of all curves change. The number of cycles that corresponds to that point is the transition life. For RT 250⁰C and 400⁰C, the experimental transition lives can be seen at table 4.7.

Table 4.7 Comparison of Experimental Transition Lives

	Experimental Data
RT	10390 – 10650 cycles
250⁰C	11630 – 13750 cycles
400⁰C	14750 – 16250 cycles

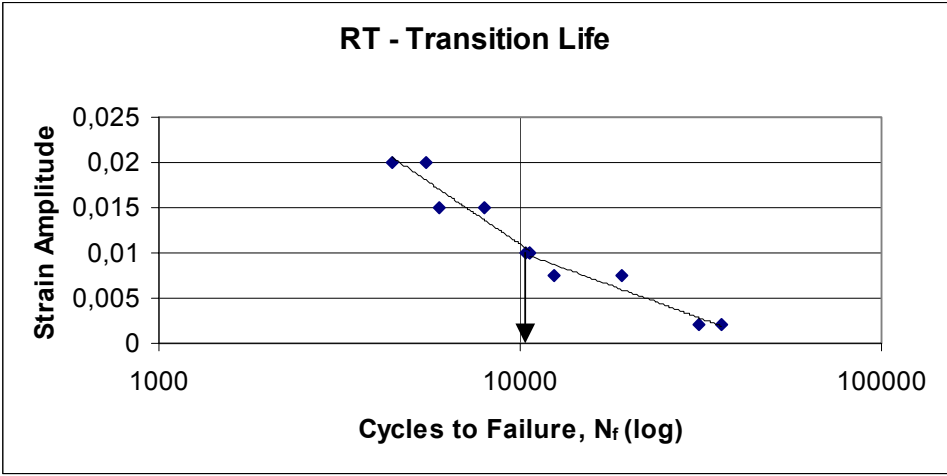


Figure 4.4 Transition Life at RT

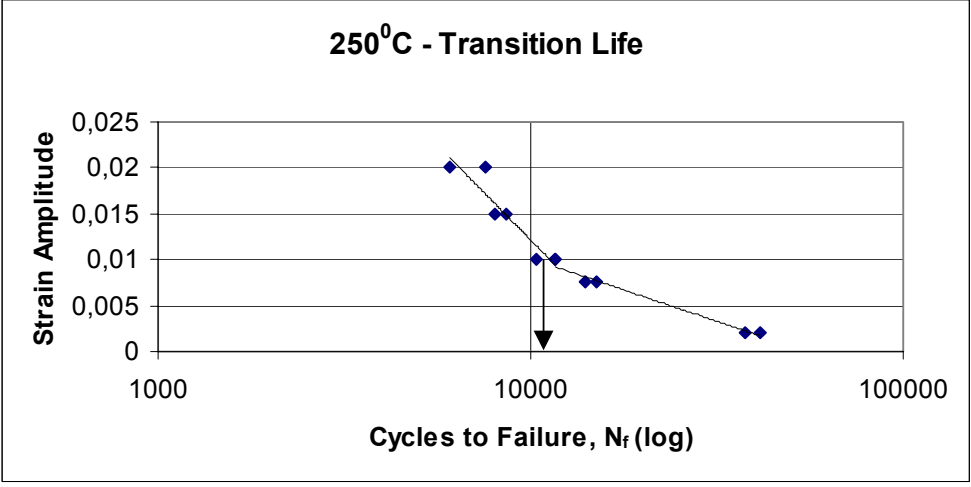


Figure 4.5 Transition Life at 250°C

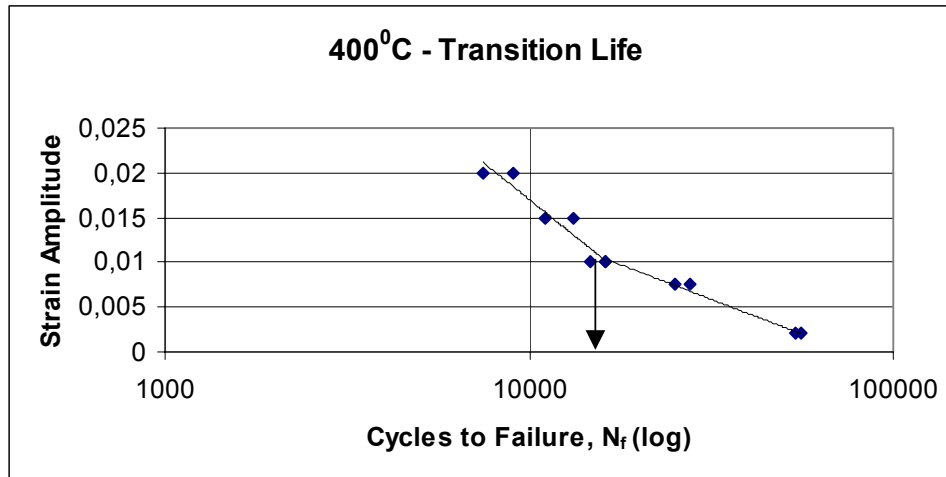


Figure 4.6 Transition Life at 400°C

4.4. Strain Amplitude versus Fatigue Life (e-N) Curves

Strain amplitude versus fatigue life curves are obtained by coinciding fatigue strength property and fatigue ductility property curves for each temperature.

4.4.1. Room Temperature e – N Curve

At room temperature, strain amplitude versus reversals to failure curve shows a typical behaviour (fig. 4.7). The transition point can be seen at the 1 % strain range. This is an expected behaviour since the transition point from elastic range to plastic range is generally seen at 0.1 strain amplitude. The total life of the material at the transition point is nearly 10390 - 10650 cycles. At 0.2 % strain, the material withstands 31380 – 36280 cycles which is the maximum value for room temperature experiments. Minimum cycles to failure occurred at 2 % strain at 4400 – 5500 cycles.

4.4.2. 250°C e – N Curve

The S – N curve for 250°C shows a slightly different property compared with the room temperature curve (fig. 4.7). The slope of both the fatigue ductility and fatigue strength lines decrease a little. The transition life is seen at 1% strain range again, but a greater value is obtained compared with the room temperature experiments (11630 – 13750 cycles). For all strain ranges of 0.2% to 2%, the material withstands greater number of cycles. Maximum life is seen at the 0.2% strain range (37860 – 41500 cycles), and minimum is seen at 2% strain range with the value of 5380 to 6220 cycles.

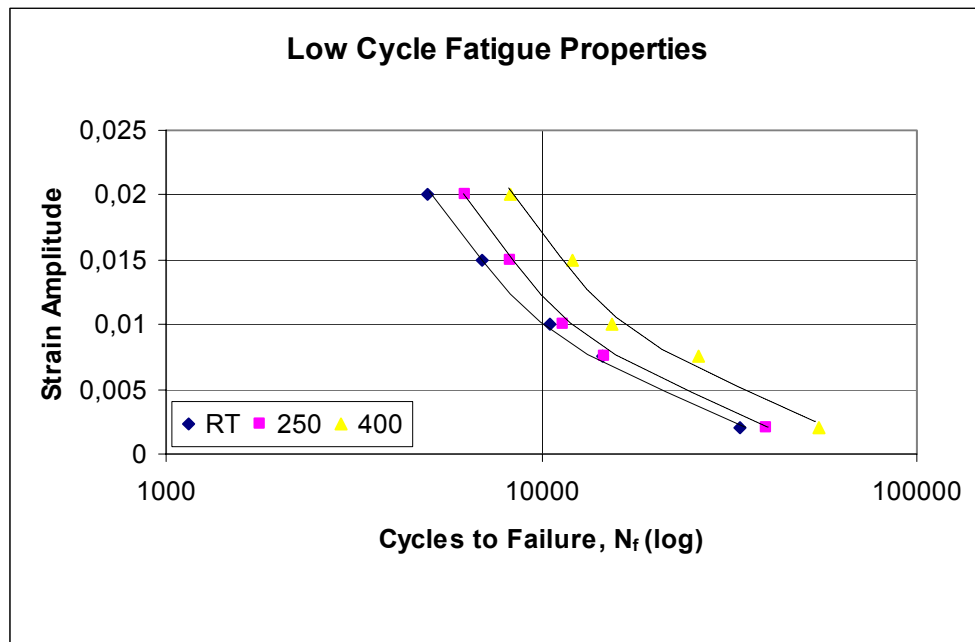


Figure 4.7 Strain - Life Curves at Three Temperatures

4.4.3. 400°C e – N Curve

Strain versus fatigue life curve obtained from 400°C experiments shows a shift to right (increasing number of cycles to failure) compared

with the room temperature and 250°C curves (fig. 4.7). For all strain ranges, the material withstands greater number of cycles. The transition life is seen at 1% strain range again, but a greater value is obtained compared with other temperatures (14750 – 16250 cycles). Maximum life is seen at the 0.2% strain range (53750 – 55660 cycles), and minimum is seen at 2% strain range with the value of 7500 to 9000 cycles.

4.5. Stress versus Fatigue Life (S-N) Curves

Fatigue performance of a material is generally analyzed in two different ways; one is fatigue life and the other is fatigue strength. The number of cycles required for a material to fail at a certain stress or strain is fatigue life. The stress at which failure occurs for a given number of cycles is the fatigue strength. At the previous chapter, it was explained with experimental results that at a given strain, fatigue life of the testing material increases with increasing temperature. From the stress point of view, the effect of temperature is observed in a different manner. The fatigue strength and fatigue life of testing material at a given maximum stress decreases with increasing temperature (fig. 4.8). The equations for those three curves could be written in the Basquin equation form as follows:

$$\sigma_{RT}=1505.7 (N_f)^{-0.0253}$$

$$\sigma_{250C}=1590.8 (N_f)^{-0.0416}$$

$$\sigma_{400C}=1339.2 (N_f)^{-0.0359}$$

Those three equations have shown that, for a given stress value, the number of cycles to failure decreases drastically with increasing temperature.

From the figure, for example at 10^4 cycles, fatigue strength of the material decreases from 1193 MPa to 962 MPa as the temperature increased from RT to 400°C. The reason of the decrease in fatigue strength with temperature could be related with the tensile properties of

the material. Tension test results have shown that the yield stress and the ultimate tensile strength values are lower at high temperatures.

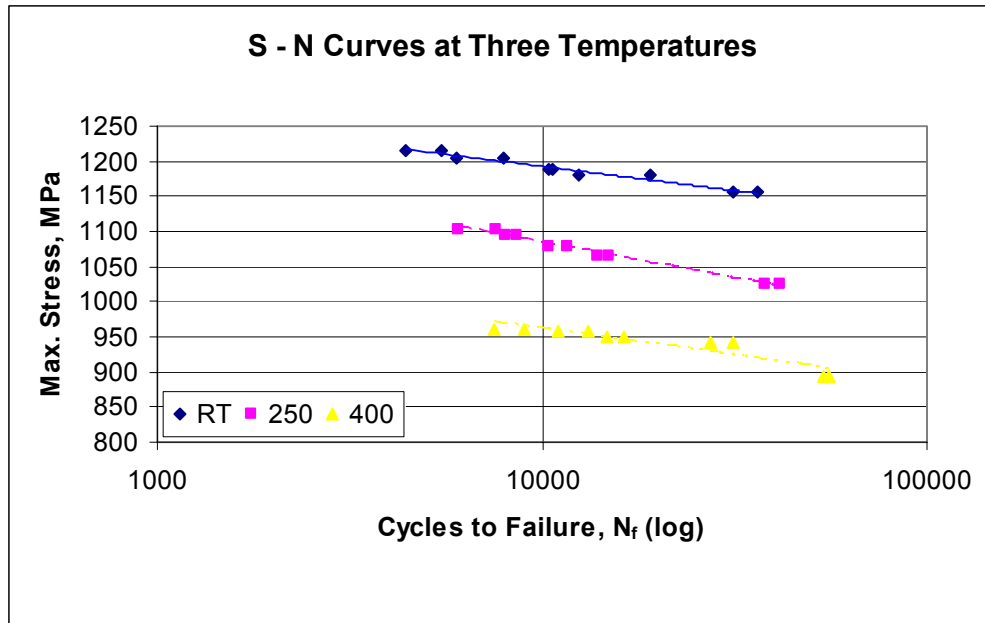


Figure 4.8 Stress - Life Curves at Three Temperatures

4.6. Effect of Temperature on Fatigue Life Results

The fatigue life of DIN 35NiCrMoV12 5 steel increases with increasing temperature up to a certain limit. As discussed in the previous chapters, the peak of fatigue life is expected to be at the range of 400°C – 450°C. Above this limit, fatigue strength will decrease rapidly.

This decrease in fatigue strength has a few reasons. One reason is the formation of surface oxide cracks above 400°C. The tips of newly formed cracks starts to oxidize and the propagation of these cracks become easier [12]. Secondly, this is the limit above which creep strength falls off more rapidly than fatigue strength and because of this, the service life of the material decrease profoundly. Another reason is the weakening

of grain boundaries at high temperatures. As the grains weaken, the transgranular type propagation of cracks changed into intergranular form. Also, internal grain cracks and oxidation of fracture surfaces occur [5]. Lastly, for tempered steels, the approaching of service temperature to tempering temperature has a great effect in the decrease of fatigue strength. In this report, the temperatures used during experiments are chosen as room temperature, 250⁰C and 400⁰C. The upper limit is determined by taking service conditions into account. It can be seen from the results listed in table 4.8 that at all strain ranges, the fatigue life of DIN 35 NiCrMoV 12 5 steel increases.

Containing molybdenum, chromium and vanadium, all of which are effective elements for an alloy to retain appreciable fatigue strength up to a certain temperature [5], DIN 35NiCrMoV12 5 steel has a high fatigue strength. The experiments show that, at constant strain, as the temperature increases the fatigue life of this material also increases (fig 4.7). From the microscopic investigations it was observed that the microstructure of the specimens after the experiments, even at high temperatures, shows no significant change (fig.4.9).



Figure 4.9 Microstructure of Specimen After Fatigue Test at 400⁰C and 0.2% Strain Amplitude (50X)

The main reason of this behaviour is either the cyclic strain hardening or relatively lower cyclic strain softening with increasing temperature. As discussed in the previous chapters, fatigue stressing may cause work – softening rather than work – hardening at room temperature. But when the temperature is increased less plastic deformation, in other words work – hardening, occurs. This decreased plastic deformation makes the steel shows less crackless plasticity at high temperatures than at room temperature. The effect of cyclic work hardening is greater at lower strain ranges. As the strain range increases, the time for hardening shortens and the effect of temperature becomes less. In other words, fatigue resistance of material increases if the applied strain is decreased.

Table 4.8 Results of all Fatigue Experiments

	25⁰C	250⁰C	400⁰C
2 % strain	4400 – 5500 cycles	6050 – 7600 cycles	7500 - 9000 cycles
1.5 % strain	5970 – 7980 cycles	8060 – 8550 cycles	11000 - 13250 cycles
1 % strain	10390 – 10650 cycles	10400 – 11630 cycles	14750 - 16250 cycles
0.75 % strain	12470 – 19120 cycles	13950 – 14940 cycles	27500 - 31250 cycles
0.2 % strain	31380 – 36280 cycles	37860 – 41500 cycles	53750 - 55660 cycles

In a recent study by R. Alain [18], a secondary cyclic hardening stage appears between 250⁰C – 450⁰C. In that temperature range, the material exhibits an improvement in the fatigue resistance. The temperatures of 200⁰C – 400⁰C corresponds to the temperature range where dynamic strain aging takes place. According to Kanazawa [19] and

Zauter et al. [20], a cyclic hardening occurs with the appearance of strain aging in the range of 200⁰C – 500⁰C.

If cyclic softening is considered for the testing material, cyclic softening effects the total life in such a way that, the amount of softening decreases as testing temperature increases. In the study of G. Bernhart , G. Moulinier, O. Brucelle and D. Delagnes [21], softening depends on the temperature and the initial total strain amplitude. According to their study, from the temperature range of 200⁰C – 550⁰C, the material (55NiCrMoV8) exhibits a cyclic strain softening. But the amount of softening decreases between the range of RT to 350⁰C. Such a behaviour also noticed in martensitic 5% chromium tool steels [22]. The initial high dislocation density which results from the quenching, decreases during cycling and generates dislocation cell structures. Size of dislocation cells is another reason of increasing fatigue life with temperature. During cyclic deformation the cell size decreases up to a certain limit with increasing temperature [7]. This decrease increases total dislocation density. As cell size decrease, dislocation multiplication and rapid locking of mobile dislocation occurs. Also, grain boundaries act as obstacles to cracks.

At the testing temperature of 400⁰C, the material withstands greater strain amplitudes without cracking. But after the formation of surface cracks, a higher crack propagation rate is expected. The reason for this behaviour is a typical phenomenon called fatigue softening. In the study of Ishii et al. [23]; during the fatigue process of materials hardened by solid solution, martensitic transformation etc., gradual elimination of obstacles such as precipitates and grain boundaries to motion of dislocations cause fatigue softening.

Manson [1] observed that cyclic hardening or cyclic softening of a material depends on the monotonic mechanical properties. The ratio of monotonic ultimate tensile strength to 0.2 % offset yield strength is the determinative factor for hardening or softening. If $\sigma_{UTS} / \sigma_{\text{offset yield}} > 1,4$

the material cyclically hardens and cyclic softening occurs if $\sigma_{UTS} / \sigma_{offset\ yield} < 1,2$. The ratios of ultimate tensile strengths to offset yield values of DIN 35NiCrMoV12 5 steel are calculated by using the values of ultimate tensile strengths and offset yield strengths for each temperature that are given at the tables 4.1, 4.2 and 4.3 at page 44. The ratios for each temperature are as follows:

$\sigma_{UTS} / \sigma_{offset\ yield}$ ratio for RT is 1,07.

$\sigma_{UTS} / \sigma_{offset\ yield}$ ratio for 250⁰C is 1,08.

$\sigma_{UTS} / \sigma_{offset\ yield}$ ratio for 400⁰C is 1,1.

From these results, it can be concluded that at all test temperatures the material cyclically softens. But, as the temperature increases, the ratio approaches to the limiting value of 1,2. These results contribute the idea of relatively less amount of cyclic softening at higher temperatures.

4.6.1. Temperature – Fatigue Life Correlation by Fatigue Damage Equations

The term ‘fatigue damage’ is often used to interpret the phenomena of fatigue failure. In the propagation of a single crack, the depth of the crack is regarded as fatigue damage [14].

The state of cracks was represented by the distribution of crack density from the outer surface to the interior of the specimen. According to Kunio, Iwamoto and Kanazawa, the state of cracks may be regarded as fatigue damage [15]. The following equations give a relationship between fatigue life and temperature.

$$D = f(k,N) \quad 4.1$$

$$k = C(T, \tau).U \quad 4.2$$

$$U = \Delta\epsilon_p. \Delta\sigma \quad 4.3$$

$$C(T, \tau) = a.\exp\left(\frac{-C_1}{T}\right) + b \quad 4.4$$

$$a = 2,1 \cdot 10^3 \cdot \tau^{0,37} \quad 4.5$$

$$b = 1 \quad C_1 = 7600$$

$$k = \{ 2,1 \cdot 10^3 \cdot \tau^{0,37} \cdot \exp(-7600/T) + 1 \} \cdot U \quad 4.6$$

$$k \cdot N_f = 4,2 \cdot 10^3 / \Delta \epsilon_p^{0,45} \quad 4.7$$

$$N_f = \frac{4,2 \cdot 10^3}{\Delta \epsilon_p^{1,45} \cdot \Delta \sigma \cdot \{ 2,1 \cdot 10^3 \cdot \tau^{0,37} \cdot \exp(-7600/T) + 1 \}} \quad 4.8$$

where;

D = state of cracks

k = variable governing factors temp, rate etc.

τ = reciprocal of strain rate

U = plastic strain energy per cycle

Table 4.9 Comparison of Exp. and Calc. Results by Damage Equations

T = RT	Experimental Cycles to Failure	Calculated Cycles to Failure
2 % strain range	4400 - 5500	2097
1,5 % strain range	5970 - 7980	3209
1 % strain range	10390 - 10650	5878
0,75 % strain range	12470 - 19120	8998
0,2 % strain range	31380 - 36280	62808
T = 250°C	Experimental Cycles to Failure	Calculated Cycles to Failure
2 % strain range	6050 - 7600	2348
1,5 % strain range	8060 - 8550	3585
1 % strain range	10400 - 11630	6559
0,75 % strain range	13950 - 14940	10076
0,2 % strain range	37860 - 41500	71510
T = 400°C	Experimental Cycles to Failure	Calculated Cycles to Failure
2 % strain range	7500 - 9000	2721
1,5 % strain range	11000 - 13250	4186
1 % strain range	14750 - 16250	7665
0,75 % strain range	27500 - 31250	11952
0,2 % strain range	53750 - 55660	86078

Although the calculated results show a similar manner with the experimental values, there are big differences between them (table 4.9). Calculated results support the experimental results in the way that an increase in the temperature of environment also increases fatigue life. But, by this equation the increasing behaviour continues and a peak in the fatigue strength would not be obtained. The difference between the experimental and calculated results occurs because of the variables (k , C_1) that contain some constants related with the material.

As a result, the correlation between temperature and fatigue life by fatigue damage equations does not give accurate results. By these equations, only the idea of increasing temperature increases fatigue life is supported.

4.6.2. Temperature – Fatigue Life Correlation by Experimental Results

The polynomial equations obtained from the experimental data give the best accommodation with the known fatigue life versus temperature relationship (fig. 4.10).

Equations Obtained From Experimental Data:

- | | |
|------------------------|--|
| 1) 0,2% strain | $N_f = 0,192.T^2 - 26,8.T + 34380$ |
| 2) 0,75% strain | $N_f = 0,2814.T^2 - 83,391.T + 17704$ |
| 3) 1% strain | $N_f = 0,0739.T^2 - 18,113.T + 10927$ |
| 4) 1,5% strain | $N_f = 0,0521.T^2 - 8,4296.T + 7153,1$ |
| 5) 2% strain | $N_f = 0,0031.T^2 + 7,4778.T + 4761,1$ |

The relationship between equations 2 - 4 and 3 - 5 shows that as the strain range decreases to a value of one half, fatigue life increases to a value of nearly twice (table 4.10). This behaviour is expected to continue until 450°C – 500°C. Then, as discussed in the previous chapters, fatigue life decreases rapidly with increasing temperature.

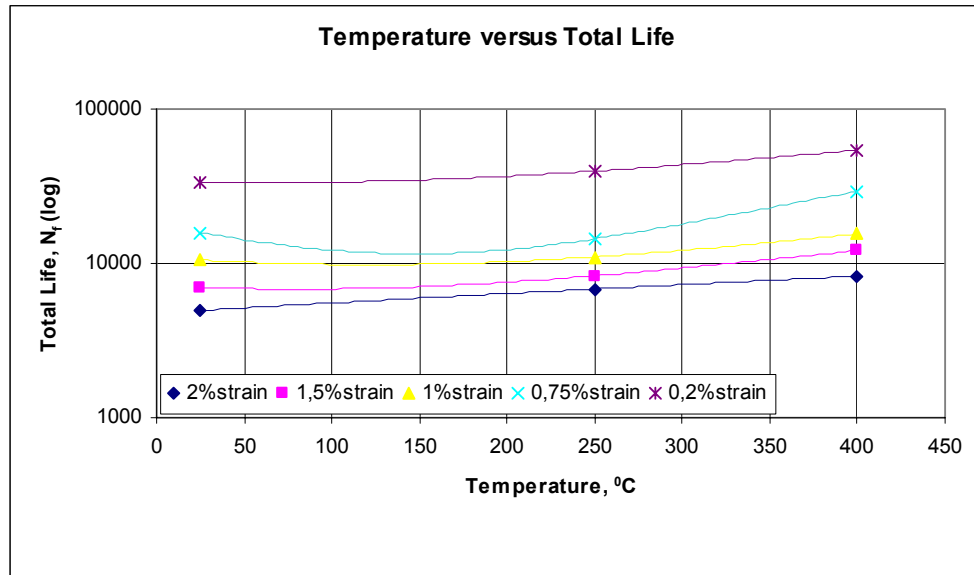


Figure 4.10 Temperature versus Total Life

Table 4.10 Fatigue Lives Calculated by Polynomial Equations

calculated cycles to failure	25 ⁰ C	250 ⁰ C	400 ⁰ C
0,2% strain	33830	39680	54380
0,75% strain	15795	14444	29400
1% strain	10520	11018	15506
1,5% strain	6975	8302	12117
2% strain	4952	6824	8248

4.7. Fractographic Results

4.7.1. Macro Inspection

Figures 4.11, 4.12 and 4.13 show the macro structure of the fractured surfaces of the specimens tested at RT, 250⁰C and 400⁰C respectively. Since the strain range is at highest value (2 % strain), several cracks are formed at the surface of the specimens (pointed in circles). These cracks could not penetrate through deeper parts of the specimens, after a small distance sudden failure occurred.

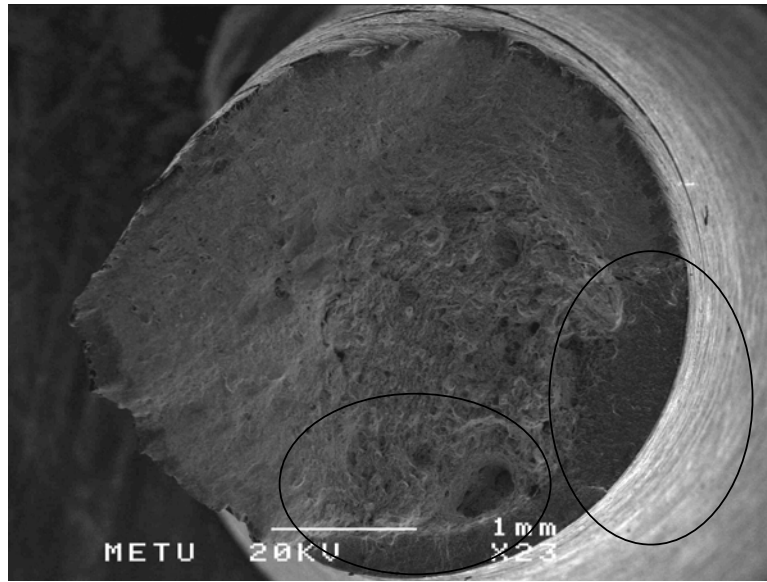


Figure 4.11 Crack Initiation Sites (encircled regions) at RT and 2 % Strain Amplitude

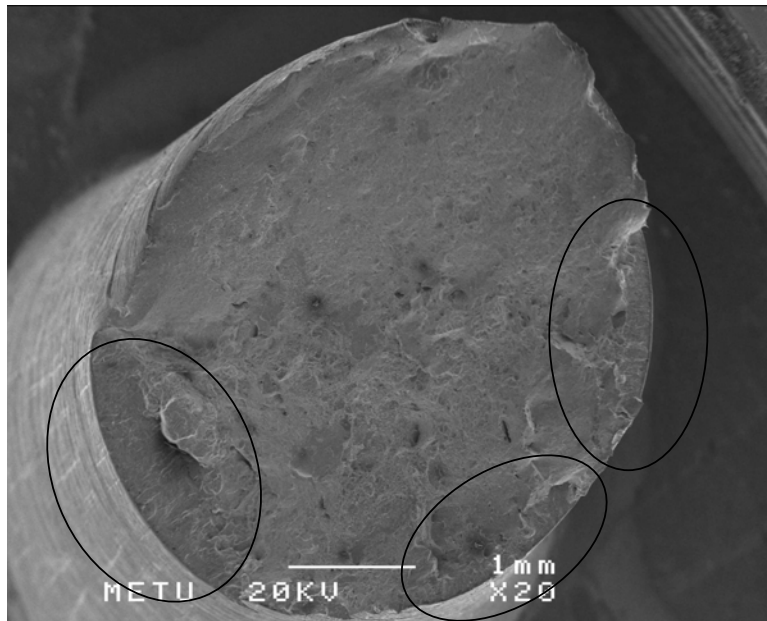


Figure 4.12 Crack Initiation Sites (encircled regions) at 250°C and 2 % Strain Amplitude

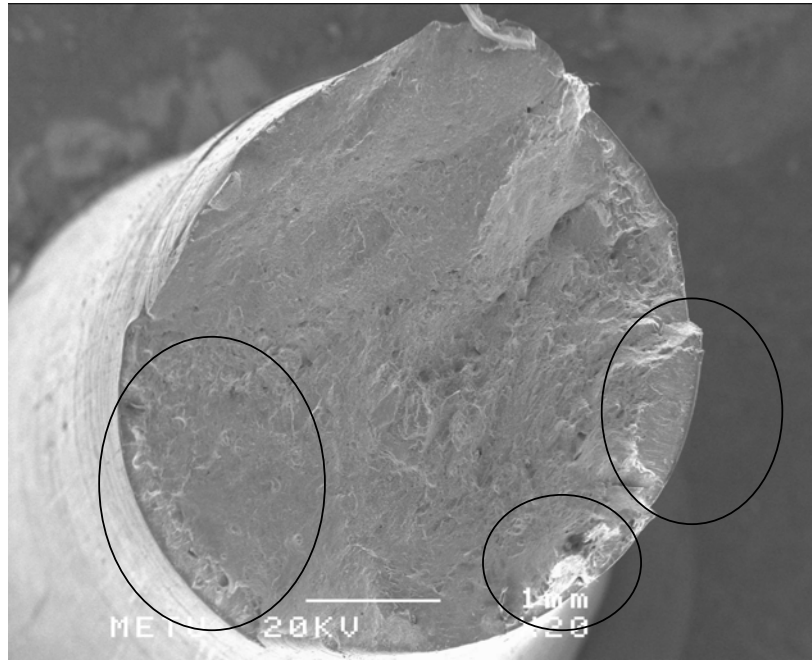


Figure 4.13 Crack Initiation Sites (encircled regions) at 400⁰C and 2 % Strain Amplitude

For the minimum strain range used in this report (0.2 % strain), the formation of cracks differs from higher strain ranges. At lower strains, only a single crack is dominant (fig. 4.14, 4.15) and the fracture occurred by the propagation of that crack (pointed in circles). Stable and unstable crack growth regions and sudden failure region can easily be seen in these figures.

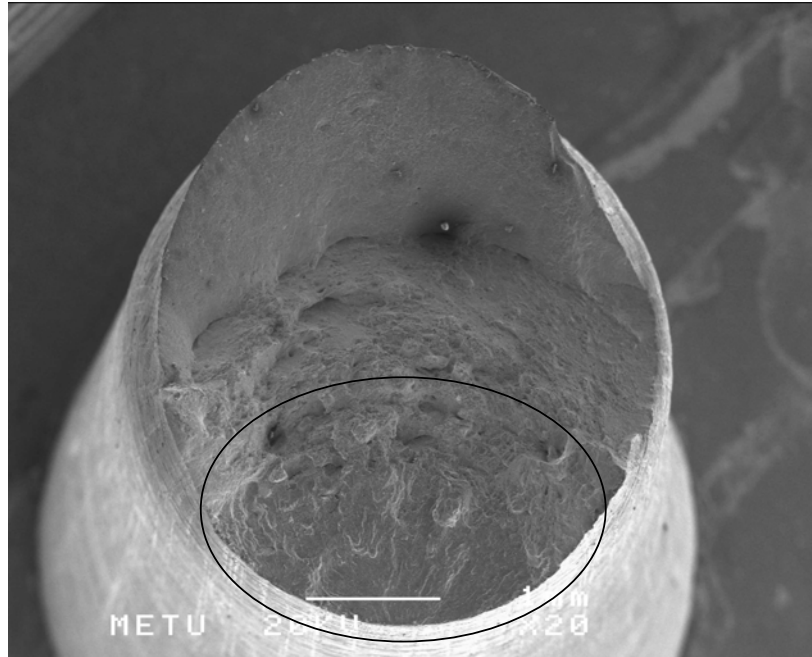


Figure 4.14 Crack Initiation Site at 250⁰C & 0.2 % Strain Amplitude

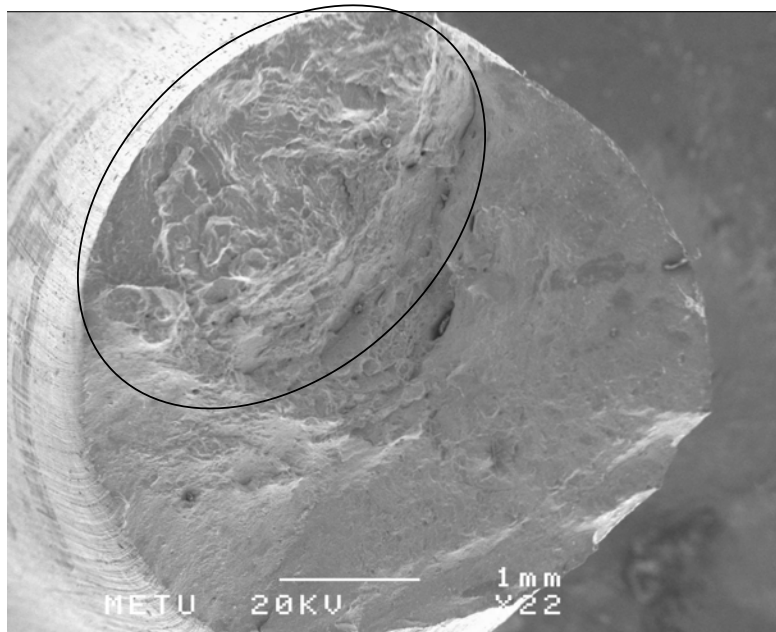


Figure 4.15 Crack Initiation Site at 400⁰C & 0.2 % Strain Amplitude

4.7.2. Micro Inspection

During the micro analyses of the fractured surfaces, typical indicators of fatigue failure such as dimples, tear ridges, stable and unstable crack growths, primary and secondary cracks and fatigue striations are observed.

Crack initiation sites can easily be observed from figures 4.16 and 4.17. Point 'a' in fig. 4.16 shows the main crack initiation site. The propagation path of that crack is along the arrow pointed with 'b'. Tear ridges are seen as white lines (point 'c'). At fig. 4.17, stage I and stage II crack growth behaviours are observed. The region stated with 'a' is the stage I area and point 'b' is the start of stage II crack growth. Point 'c' shows the river – pattern like appearances forming along the crack growth direction.

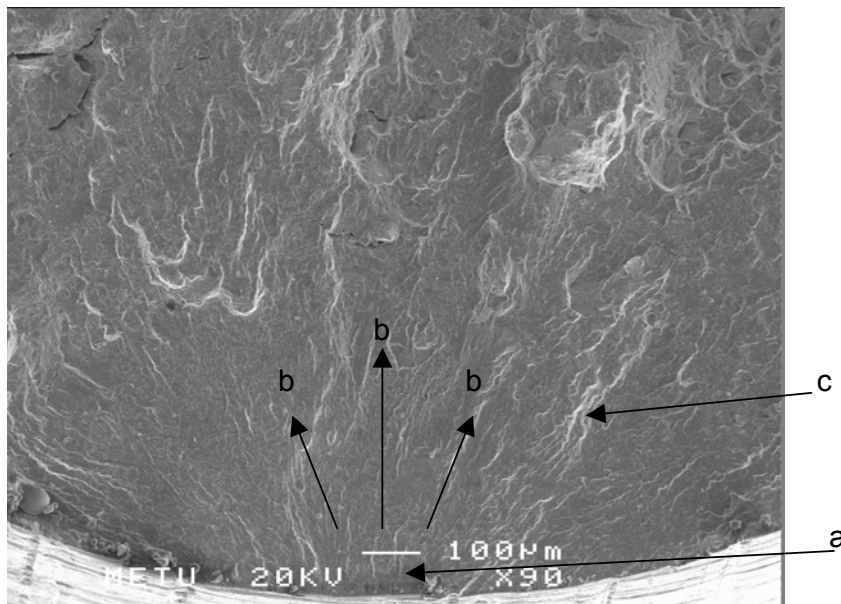


Figure 4.16 Crack Initiation at 250°C and 0.2 % Strain

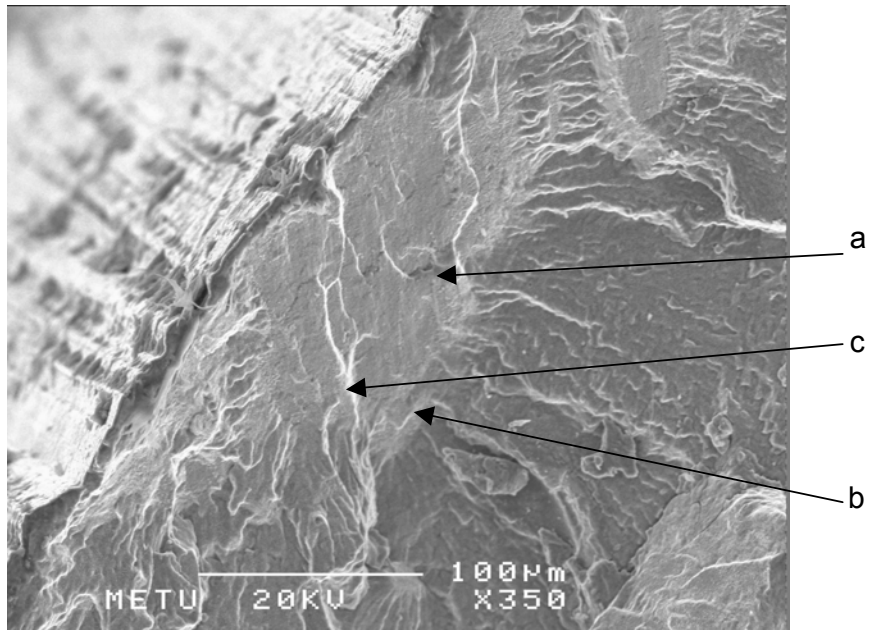


Figure 4.17 Crack Initiation at 400⁰C and 0.2 % Strain

At the following figure (fig. 4.18), the white patterns (pointed with 'a') are called the tear ridges. This fatigue indicator shows the direction of the propagation (crack growth direction is shown on the figure). The penetration of tear ridges can be described as opposite of branching (joining of small branches). Point 'b' shows a secondary crack which are generally form perpendicular to the tear ridges.

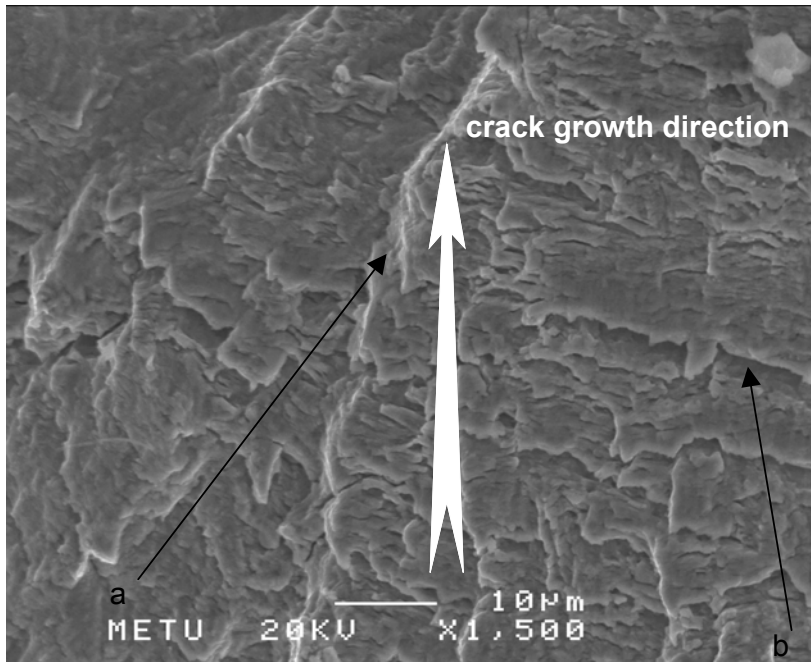


Figure 4.18 Tear Ridges and Secondary Crack at 250⁰C and 0.2 % Strain

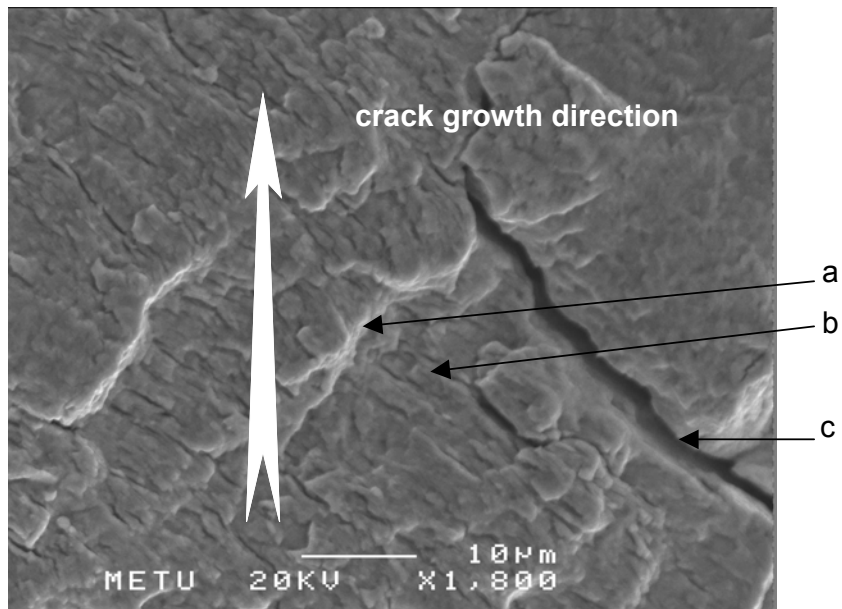


Figure 4.19 Striations and Secondary Cracks at 250⁰C and 2 % Strain

Figure 4.19 shows tear ridge and secondary crack pointed by 'a' and 'c' respectively. The indicators marked with 'b' are fatigue striations that occur at every single cycle. Crack growth direction is perpendicular to both the secondary cracks and the striations. By using those striations, the growth rate can be calculated. A closer view of striations can be seen at fig. 4.20. The crack growth rate for point 'a' is nearly $1.3\mu\text{m}/\text{cycle}$ at 250°C at a strain range of 2 %. At 400°C the rate is about $2.5\mu\text{m}/\text{cycle}$ (point 'a' on fig.4.21). In order to obtain an overall growth rate, the whole surface of the crack propagation region must be considered and an average value of the striation spacings must be calculated.

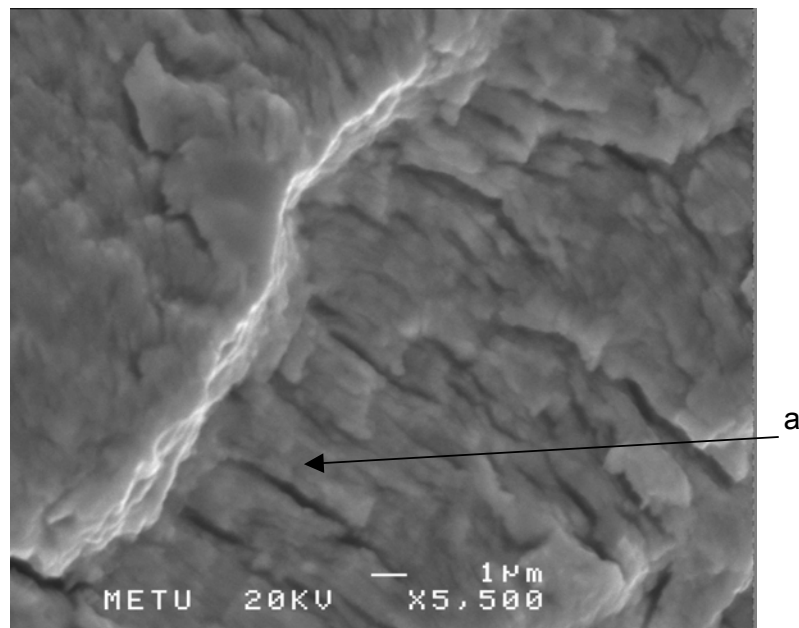


Figure 4.20 Striations Formed at 250°C and 2 % Strain

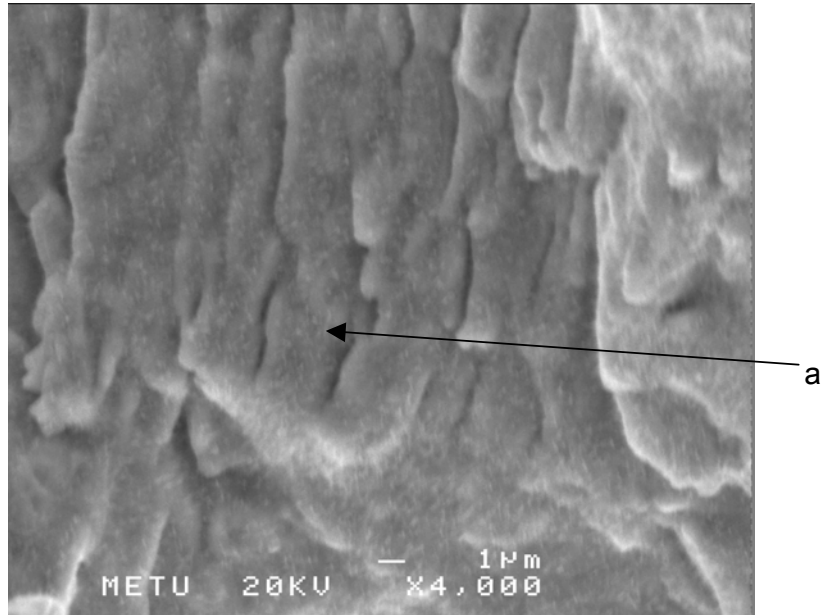


Figure 4.21 Striations Formed at 400⁰C and 2 % Strain

Dimples which have sponge-like structure are seen in the fast fracture region. Figure 4.22 and 4.23 show typical examples of the fast fracture region. For all temperatures and strain ranges, the formation of dimples are similar. So temperature has no effect on the formation of dimples.

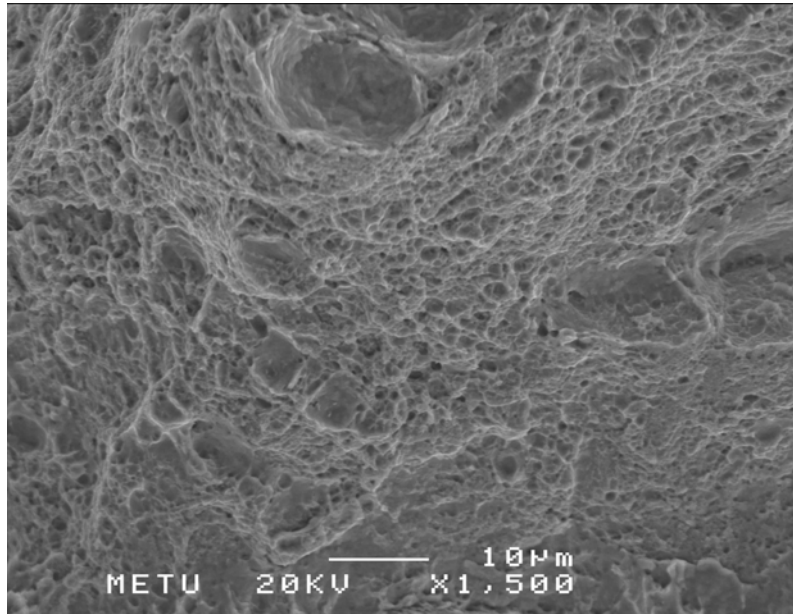


Figure 4.22 Dimples Formed at 250°C and 0.2 % Strain

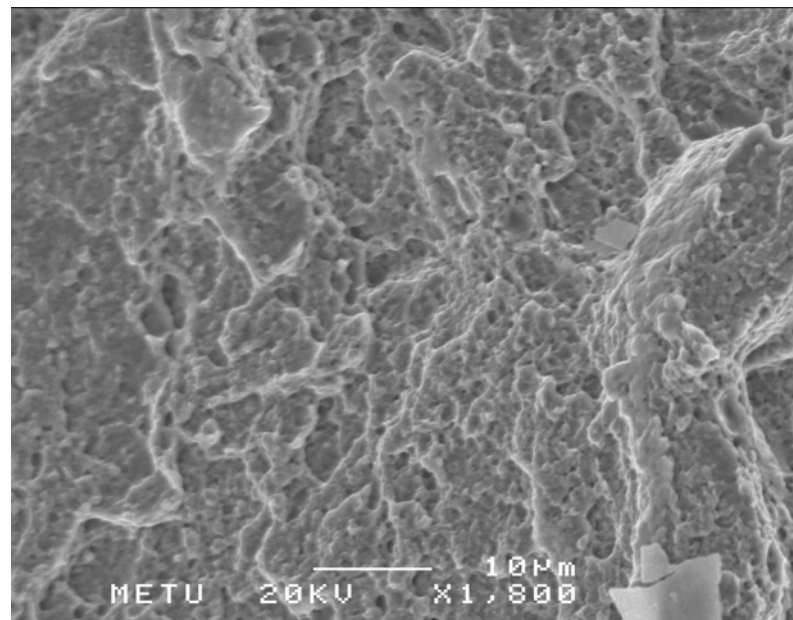


Figure 4.23 Dimples Formed at 400°C and 0.2 % Strain

CHAPTER 5

CONCLUSIONS

- (1) As temperature increases, fatigue life at a given strain amplitude also increases thus, at 400⁰C, the maximum fatigue life is reached.
- (2) Fatigue strength and fatigue life at a given stress amplitude are inversely proportional with temperature. They, do decrease with increasing temperature.
- (3) The effect of temperature on the transition life is negligible.
- (4) At low strain amplitudes, a single crack initiates and causes failure. As the applied strain is increased, an increase in the number of crack initiation sites is observed. The length of those cracks is shorter compared with the single crack that formed at lower strains.

REFERENCES

1. Deformation and Fracture Mechanics Of Engineering Materials - Hertzberg, Richard W. – John Wiley & Sons 1996.
2. Yield Point Phenomena in Metals and Alloys – E. O. Hall – Plenum Press New York 1970.
3. Materials Science and Engineering, an Introduction 3rd ed. - Callister, William D. Jr. - New York: John Wiley & Sons, Inc., 1994.
4. Mechanics of Materials 2nd ed. - Beer, Ferdinand P., and E. Russell Johnston, Jr. - New York: McGraw-Hill, Inc. 1992.
5. Fatigue Of Metals – Forrest, Peter George – Owford, New York, Pergamon Press, 1962.
6. Metal Fatigue – J.A. Pope (ed.) – London, Chapman & Hall LTD. 1959.
7. Fatigue At Elevated Temperatures - H. Abdel-Raouf, T.H. Topper, and A. Plumtree – A.E. Carden, A.J. McEvily, and C.H. Wells (ed.) – ASTM Special Technical Publication 520, 1972.
8. Fatigue At Elevated Temperatures - J. Wareing, B. Tomkins, and G. Sumner – A.E. Carden, A.J. McEvily, and C.H. Wells (ed.) – ASTM Special Technical Publication 520, 1972.
9. Manual On Low Cycle Fatigue Testing – Raske and Morrow - R.M.Wetzel, Ford Motor Co., L.F. Coffin,Jr. (ed.) - ASTM Special Technical Publication 465, 1969.
10. Standard Practice For Strain – Controlled Fatigue Testing - ASTM Designation : E 606 – 92.

- 11.** Standard Test Methods for Tension Testing of Metallic Materials (Metric) - ASTM Designation : E 8 M - 93.
- 12.** Fatigue And Fracture - ASM Handook Volume 19.
- 13.** Structure and Properties of Engineering Alloys – William F. Smith – McGrow & Hill Publishing Co. 1981.
- 14.** Trans. Japan Soc. Mech. Engr., Volume 30, p. 215, 780 – Simizu, M., Hachuno, K., Nakamura, H. & Kunio, T.
- 15.** Fracture 1969 – P. L. Pratt (editor in chief) – Behaviour of Low Cycle Fatigue at Elevated Temperatures - Kunio, T., Iwamoto, K., Kanazawa, K.
- 16.** Fundamentals of Cyclic Stres and Strain – Bela I. Sandor - McGrow & Hill Publishing Co. 1974.
- 17.** Defects, Fracture and Fatigue – G. C. Sih, J. W. Provan (editors) – Martinus Nijhoff Publishers.
- 18.** Low cycle fatigue behaviour in vacuum of a 316L type austenitic stainless steel between 20 – 600^oC – R. Alain, P. Violan, J. Mendez – Materials Science and Engineering A229 (1997) 87-94.
- 19.** Low Cycle Fatigue – K. Kanazawa, K. Yamaguchi, S. Nishijima – ASTM-STP 942, 1998, pp. 519-530.
- 20.** R. Zauter, F. Petry, M. Bayerlein, C. Sommer, M.J. Christ, H. Mughrabi – Philos. Mag. A, 66 (3) (1992) 425-436.
- 21.** High temperature low cycle fatigue behaviour of a martensitic forging tool steel - G. Bernhart, G. Moulinier, O. Brucelle, D. Delagnes - International Journal of Fatigue 21 (1999) 179–186
- 22.** Chai H, Fan Q. Proceedings of the 5th International Conference on Fatigue and Fatigue Thresholds, 1993:195.
- 23.** Low cycle fatigue properties of 8Cr-2WVTa ferritic steel at elevated temperatures - T. Ishii, K. Fukaya, Y. Nishiyama, M. Suzuki, M. Eto - Journal of Nuclear Materials 258-263 (1998) 1183-1186.
- 24.** The Effect of Temperature on The Low Cycle Fatigue Properties of a 15Cr-15Ni, Ti Modified Austenitic Stainless Steel - R. Sandhya, K. Bhanu Sankara Rao, and S.L. Mannan - Scripta Materialia, Vol. 41, No. 9, pp. 921–927, 1999.